Journal of Natural Gas Science and Engineering 8 (2012) 68–84

Contents lists available at SciVerse ScienceDirect

Journal of Natural Gas Science and Engineering

journal homepage: www.elsevier.com/locate/jngse

Comparative sequence stratigraphy and organic geochemistry of gas shales: Commonality or coincidence?

Roger M. Slatt [a], Norelis D. Rodriguez [b,*]

[a] Institute of Reservoir Characterization and School of Geology and Geophysics, University of Oklahoma, 100 E. Boyd St., Norman, OK 73072, USA
[b] Chevron Energy Technology Co., Exploration & New Ventures, 1500 Louisiana St., Room 28154, Houston, TX 77002, USA

ARTICLE INFO

Article history:
Received 14 October 2011
Accepted 19 January 2012
Available online 15 February 2012

Keywords:
Shale
Shale sequence stratigraphy
Shale gas geochemistry
Gas shales

ABSTRACT

Comparison of some Paleozoic and Mesozoic gas shales has revealed a generally common sequence stratigraphy, consisting of, from the base upward: combined sequence boundary/transgressive surface of erosion (SB/TSE) upon which sits a transgressive systems tract (TST) enriched in organic matter, then a somewhat 'cleaner gamma-ray' highstand or regressive systems tract (HST/RST). When resolvable, this stratigraphy occurs at 2nd, 3rd, and 4th order relative sea level cyclicity, forming couplets of relatively organic-rich (TST and condensed section-CS) and organic-poor (HST/RST) strata at these time scales. A higher order sequence stratigraphy can be developed for Mesozoic shales than for Paleozoic shales owing to greater biostratigraphic age resolution of the former. The higher frequency cycles are superimposed upon lower frequency cycles, giving rise to a complex stratigraphy of several couplets of differing thickness and distribution. These documented common characteristics provide the basis for a unifying, general sequence stratigraphic model for shales which can be utilized to identify, predict and map the most productive facies within a shale stratigraphic interval.

There also are several commonalities in geochemistry of gas shales. Prolific gas shales are usually >200 ft (65 m) thick, contain >3% TOC, have Hydrogen Index values >350 mg HC/g, contain Type II kerogen and have organic maturity values >1.1% Ro. Organic-rich shales typically contain minerals such as pyrite and phosphates (apatite) and show biomarker ratios (pristane/phytane, steranes distribution, C_{13}–C_{20} regular isoprenoids and C_{18} aryl isoprenoids) indicative of anoxic conditions during source rock deposition. In high maturity areas, there is a reversal in ethane isotope abundance owing to secondary cracking of hydrocarbons; such a reversal is normally associated with best gas production. Relative hydrocarbon potential (S1 + S2/TOC) is a geochemical parameter which reflects oxygenation conditions in the depositional environment. It can be related to relative sea level fluctuations within a sequence stratigraphic context.

Understanding the sequence stratigraphy of shale provides a powerful tool not only for regional-to-local stratigraphic correlations from well logs and seismic reflection records, but also for high-grading stratigraphic intervals most favorable for preservation of organic matter and gas generation and storage.

1. Introduction

Increased interest in global unconventional gas shales as a major, long-term energy source has led to a plethora of recently published (and unpublished) scientific and technical studies, workshops and conferences. In this paper, we address two important areas of study—sequence stratigraphy and petroleum geochemistry. Specifically, we summarize important new (e.g. *Stratigraphy*- (Bohacs, 2010; Lash and Engelder, 2011; Slatt et al., in press-a) *Geochemistry*- (Ferworn et al., 2008; Zumberge et al., 2009) which have brought attention to stratigraphic and geochemical commonalities among gas shales, suggestive of a unifying stratigraphic model for their origin, distribution, and gas (and oil) resource potential. We also provide examples of how and why stratigraphic and geochemical characteristics can be linked.

2. Basic principles

Traditional sequence stratigraphic principles and analysis (Van Wagoner et al., 1990) have now been applied to many of the major gas shales; these studies are referenced and summarized below. Sequence stratigraphy is based upon the premise that

* Corresponding author.
E-mail addresses: rslatt@ou.edu (R.M. Slatt), norelis@chevron.com (N.D. Rodriguez).

1875-5100/$ – see front matter © 2012 Elsevier B.V. All rights reserved.
doi:10.1016/j.jngse.2012.01.008

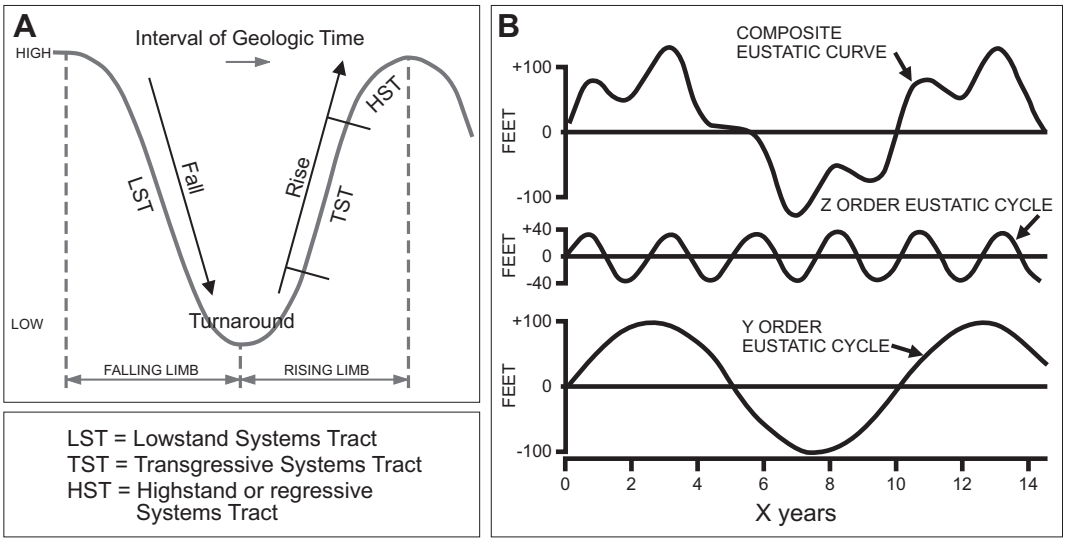

Fig. 1. (A) Relative sea level cycle showing the positions on the curve of lowstand, transgressive and highstand systems tracts. (B) Cycles at different time intervals (X years) occur simultaneously (for example cycles with frequence of Y and Z years of geologic time) a composite sea level curve results, which controls the nature of depositional environments and deposition of shale (and other) facies. See text for an explanation of the scales of cyclicity within geologic time frames.

through geologic time, the oceans have risen and fallen in a cyclic manner (i.e. rise and fall of sea level) (Fig. 1A). A relative sea level cycle consists of: (1) a falling and turnaround stage, in which Lowstand Sytems Tract (LST) strata are deposited, (2) and a rising stage, first exhibiting a rapid rate of rise in relative sea level, in which Transgressive Systems Tract strata are deposited, and a later, slower rate of rise, in which Highstand or Regressive Systems Tract strata are deposited (Figs. 1 and 2). The term 'relative' is used

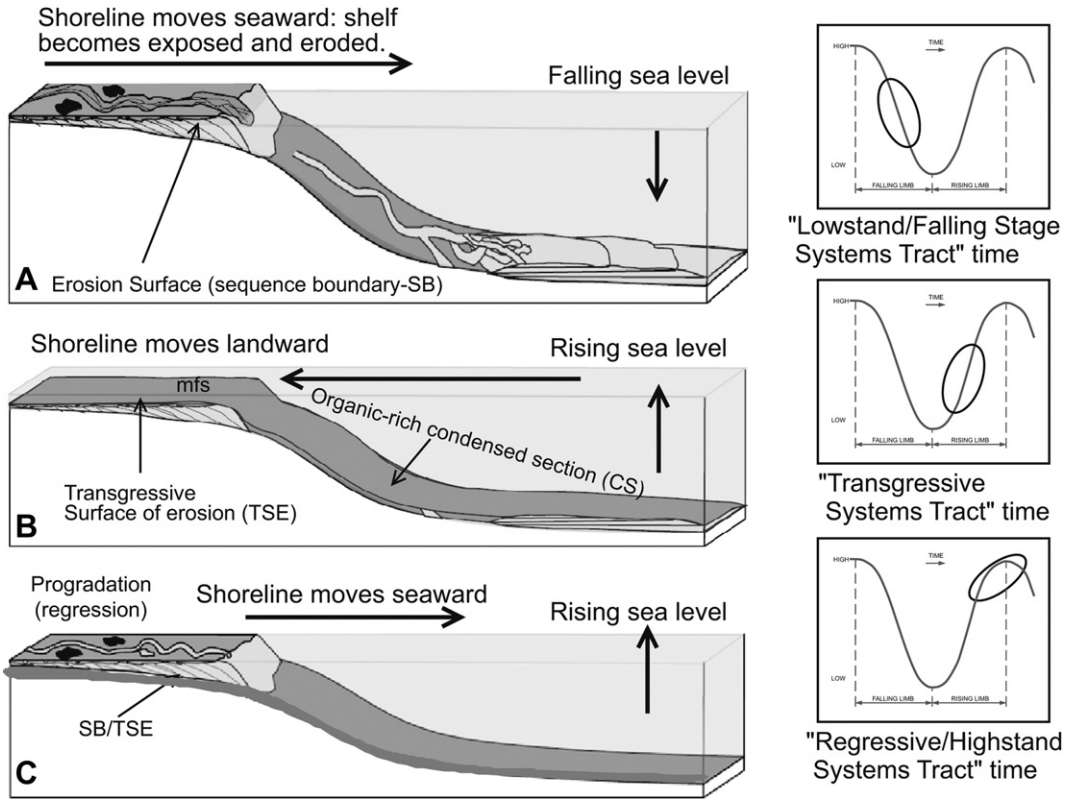

Fig. 2. Stages of sea level relative to depositional and erosional processes. (A) shows the position of the sea surface and shoreline during a falling stage of relative sea level; at this time shallow marine environments become subaerially exposed and eroded, generating a sequence boundary (SB). Eroded strata are transported and deposited in deeper water. (B) shows the position of the sea surface during a rise in sea level; at this time, the shoreline migrates landward across the sequence boundary, further eroding it and producing a transgressive surface of erosion (TSE) (combined with the earlier formed sequence boundary) and an organic-rich, condensed section (CS), capped by a maximum flooding surface (mfs) is deposited over a large area of the shallow to deeper marine environment. (C) shows the seaward movement of the shoreline during the waning stages of sea level rise; at this time, sediment is deposited in sufficient volume to fill accommodation space on the shelf, so the shoreline is pushed (i.e. progrades) seaward. The three inset sea level curves show the three environments during falling and rising sea level [ovals denote the falling stage (A), relatively rapid rise (B), and slower rise (C)].

because the change in sea level may be due to eustatic, climatic, and/or tectonic causes as well as the rate of sea level change relative to the rate of sediment supply, all of which are often difficult to differentiate or apportion (Van Wagoner et al., 1990).

Typical time frames in which sea level cycles (length of geologic time for a complete lowstand–highstand of relative sea level) can be interpreted for shales (mainly based upon their fossil components) include: 2nd order = approximately 10–25 My; 3rd order = approximately 1–3 My; 4th order = approximately 100,000–300,000 years. Mesozoic and Cenozoic shales often have a more detailed biostratigraphic age zonation than do Paleozoic shales, owing to the greater abundance of age-datable fossils in the younger rocks.

These scales of relative sea level cyclicity occur simultaneously, thus leading to a composite sea level curve (Fig. 1B) which provides for significant variability in depositional environments, the timing of deposits and their ultimate stratigraphy (stacking) and lateral continuity.

Abbreviations common to sequence stratigraphy (Van Wagoner et al., 1990), and used throughout this paper include: SB = *sequence boundary*; TSE = *transgressive surface of erosion*; RSE = *regressive surface of erosion*; LST = *lowstand (falling stage) systems tract*; TST = *transgressive systems tract*; RST = *regressive systems tract* (which in this paper we consider analogous to HST or *highstand systems tract*); CS = condensed section; mfs = *maximum flooding surface*; mrs = *maximum regressive surface*; TOC = *total organic content* (wt. %).

3. Comparative sequence stratigraphy

Below we present the basic sequence stratigraphy of common gas shales, taking into account the composite cyclicity of relative sea level change and its affect upon stacking patterns and stratigraphy.

3.1. The Devonian ***Marcellus Shale,*** north-eastern US*A* was deposited as a 2nd order sequence in the Appalachian foreland basin (Fig. 3). It is divided into a lower Union Springs Member and an upper Oatka Creek Member, both of which are separated by the Cherry Valley Member. The Union Springs member sits upon a SB/TSE. Lash and Engelder (Lash and Engelder, 2011) interpret the Union Springs Member as a 3rd order depositional sequence composed of a lower, upward-increasing API gamma-ray TST and an upper, upward-decreasing API gamma-ray RST, with a mfs constituting the highest gamma-ray shale (Fig. 3). The Oatka Creek Member comprises another 3rd order sequence consisting of a basal RSE, a relatively thin, mainly limestone TST and a thicker RST (Fig. 3). TOC values range up to about 10 wt. % and track gamma-ray values in the well shown in Fig. 3, but in some wells can be as high as 20 wt. % (Lash and Engelder, 2011; Bowker and Grace, 2010; Boyce et al., 2010). Quartz content ranges 40–75% and clay is 10–45% (Boyce et al., 2010). Quartz occurs as a combination of detrital silt with associated diagenetic overgrowths, cryptocrysalline replacement of fossil

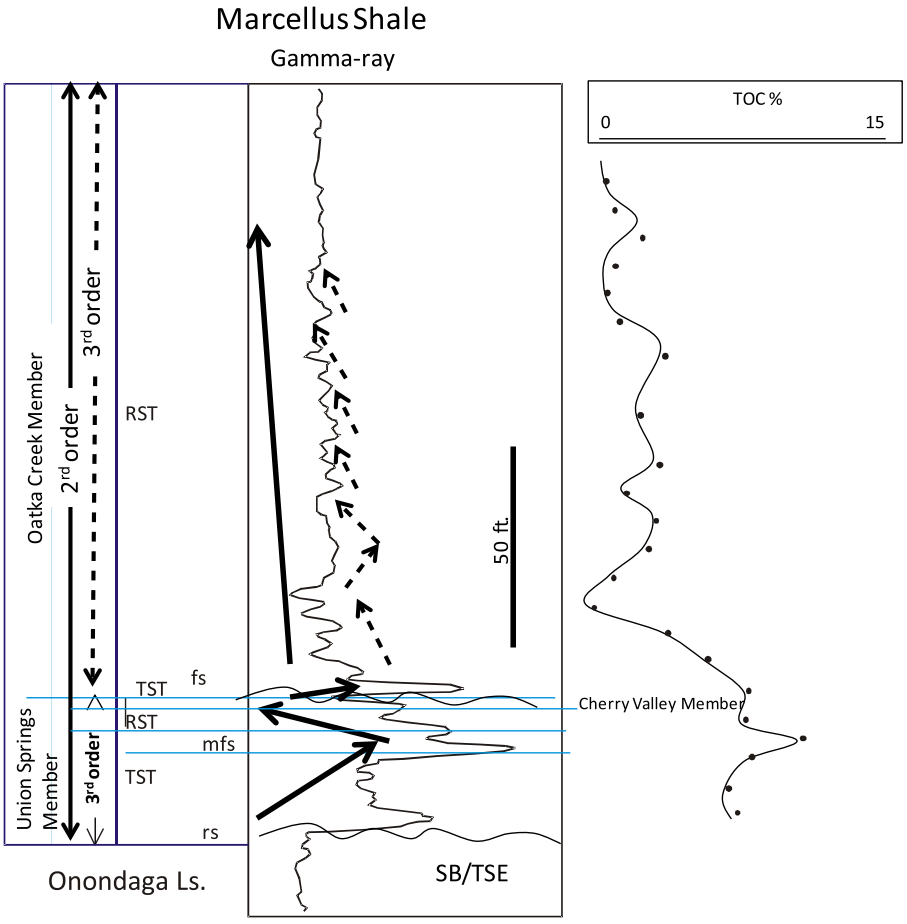

Fig. 3. Gamma-ray and Total Organic Carbon (TOC) profiles of the Marcellus Shale, showing 2nd and 3rd order sequence stratigraphy. Modified from Bowker and Grace (Bowker and Grace, 2010) and Lash and Engelder (Lash and Engelder, 2011; Fig. 20). In this, and subsequent figures, solid arrows denote progressive upward increase and decrease of API gamma-ray counts of a stratigraphic interval at the lower order scale of cyclicity and the dashed arrows denote progressive upward increase and decrease of API gamma-ray counts of a stratigraphic interval at the higher order scale of cyclicity (i.e. 2nd vs. 3rd order cyclicity, etc.). A general TOC trend curve is overlain upon the actual measured TOC values (dots).

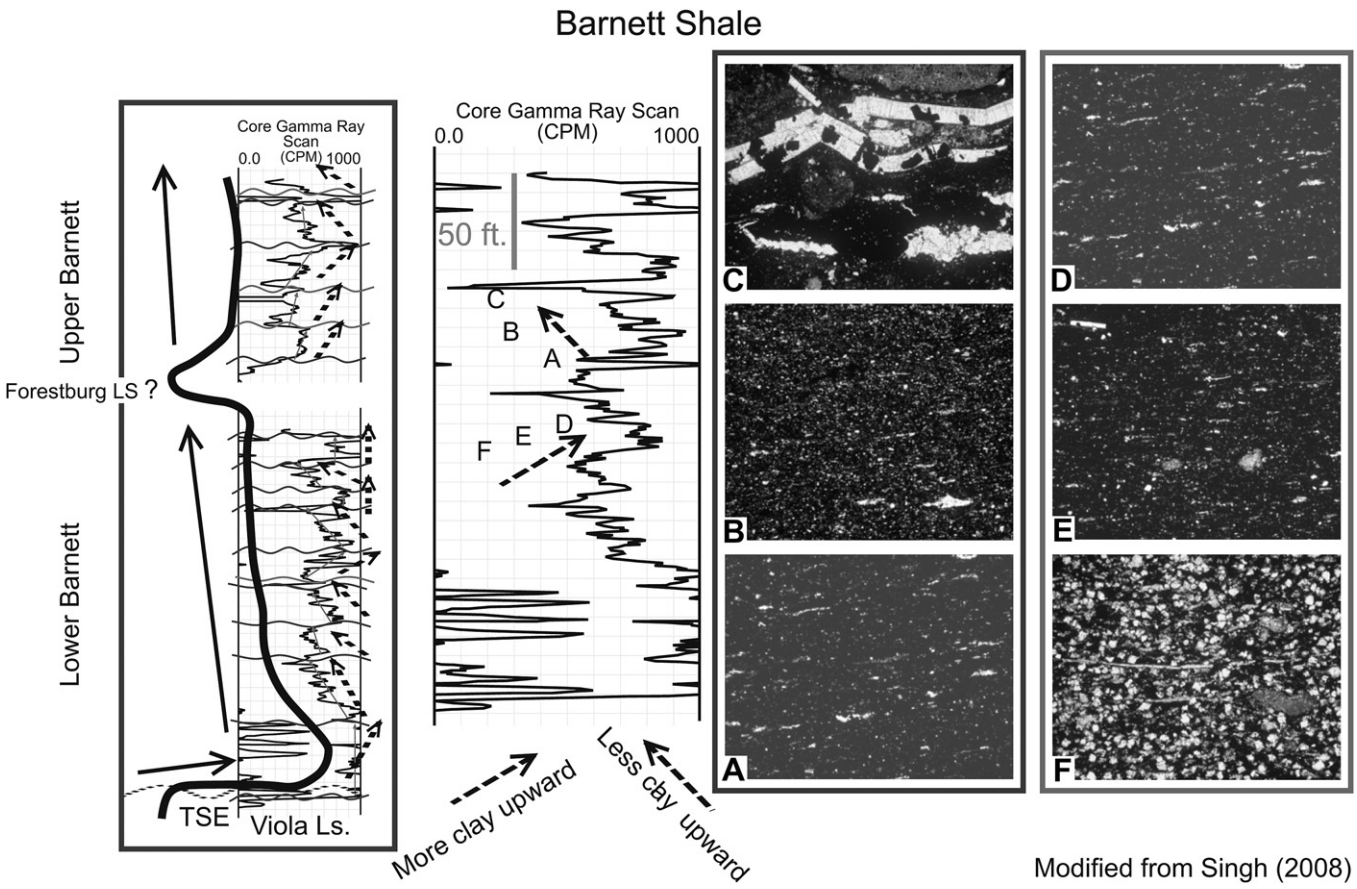

Fig. 4. Core gamma-ray scans of complete (left) and partial (right) stratigraphic profiles of the Barnett Shale in the northern Fort Worth Basin (modified from Singh (Singh, 2008) and Slatt et al (Slatt et al., in press-a). The solid black curve and corresponding solid arrows correspond with a 2nd order stratigraphic sequence for the entire Barnett Shale, and the two dashed arrows highlight two of the several 3rd order sequences which comprise the Barnett Shale (Singh, 2008). Thin section photomicrographs A, B, and C show the progressive upward change from a lower clay-organic rich lithofacies (A), to a more quartzose-clay lithofacies (B), to a shelly-carbonate lithofacies (C), which correspond to a 'cleaning upward' API gamma-ray log pattern. Thin section photomicrographs D, E, and F show a progressive upward change from a lower dolomitic mudstone (F), to a calcareous mudstone (E), to a clay-organic rich lithofacies, which correspond to a 'dirtying upward' API gamma-ray log pattern.

fragments, and pore-filling cement (Laughrey et al., 2010), which give rise to relatively high quartz content within parts of the TST. Quartz, pyrite, and detrital and authigenic calcite provide potential brittleness to these rocks. Less brittle (i.e. more ductile) rocks are those with abundant detrital and pore-filling authigenic clays and TOC (Lash and Engelder, 2011).

3.2. The Devonian ***Barnett Shale*** was deposited over an approximate 22 My time interval in the Fort Worth (Texas, USA) foreland basin. It is divided into lower and upper Barnett Shale intervals separated in the northern part of the basin by the Forestburg Limestone, which pinches out toward the southwest (Figs. 4 and 5). The lower Barnett sits atop a SB/TSE which

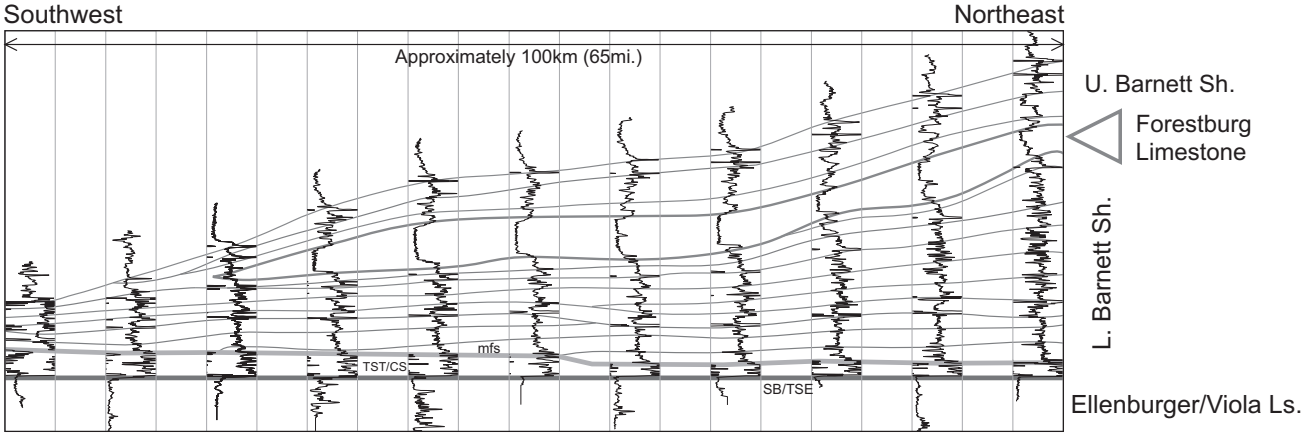

Fig. 5. Approximate 100 km (65 mi) long stratigraphic cross section of the Barnett Shale datumed on the TST/CS/mfs. Note the downlap pattern of the Forestburg Limestone and individual 3rd order sequences onto the mfs, indicating much of the Barnett Shale is a 2nd order transgressive-highstand deposit.

caps the underlying Viola/Ellenburger limestones (Fig. 4). The lower Barnett is dominated by siliceous mudstones and the upper Barnett is dominated by calcareous mudstones; other lithofacies include phosphatic mudstones, spiculitic turbidites, micritic and cross-laminated limestones, and calcareous concretions (Slatt et al., in press-a; Singh, 2008; Abouelresh and Slatt, 2012). These lithofacies form distinctive stacking patterns, termed 'gamma-ray parasequences' (GRP) by Singh (Singh, 2008) in the northern Ft. Worth basin, and termed 'high frequency-sequences' by Abouelresh and Slatt (2012) in the southern part; 12-14 such sequences occur in different wells. Collectively, they represent 3rd order relative sea level cycles superimposed upon one (lower Barnett) or two (lower and upper Barnett) 2nd order cycles (Fig. 4). The sequences downlap toward the southwest onto the SB/TSE (Fig. 5). Detrital quartz, calcite, and clays (illite; illite/smectite) are the main inorganic constituents. Biogenic components include siliceous sponge spicules, agglutinated foraminifera, *Tasmanites* cysts, and fecal pellets (Slatt and O'Brien, 2012). In most wells, TOC ranges up to about 10 wt. % and tracks API gamma-ray values. The Barnett extends westward into the less-drilled Delaware Basin (west Texas), where it overlies Mississippian Lime and Chert in different parts of the basin. Similar facies occur in the Delaware Basin, although sometimes in different proportions than in the Fort Worth Basin.

3.3. The upper Devonian–lower Misissippian ***New Albany Shale*** was deposited over a 20 My time interval in the Illinois Basin, USA (states of Illinois, Indiana, and Kentucky). It consists of a variety of interbedded organic-rich and organic-poor shale facies with minor dolomite and sandstone. Some shales are pyritic and others are siliceous, A high frequency sequence stratigraphic framework has been developed by Bohacs and Lazar (Bohacs, 2010), consisting of 10 systems tracts within 4 SB-bounded depositional sequences which reveal a downlap pattern onto the basal SB/TSE (Fig. 6). These systems tracts give rise to systematic alternations of organic-rich TST and organic-poor LST/HST shales (Fig. 6).

3.4. The Late Devonian–Early Mississippian ***Woodford Shale*** was deposited in the Anadarko–Arkoma–Ardmore basins, central USA over a 33 My (359–392 My) time span (Paxton et al., 2006). It is comprised of three members: the Lower Woodford black shale which unconformably (SB/TSE) overlies Hunton Group carbonates, the Middle Woodford organic-rich, black, pyritic shale, and the more quartzose-phosphatic Upper Woodford (Fig. 7). Stratigraphic studies of the Woodford by drilling a borehole at and just behind a quarry wall (Wyche Farm quarry; (Slatt et al., in press-b)) have provided excellent correlation with subsurface wells for improved understanding of both subsurface stratigraphy and natural fracture distribution (Fig. 7). The Woodford Shale was deposited during a 2nd order sea level cycle, but a superimposed 3rd order sequence stratigraphic framework has been developed at the Henryhouse Creek outcrop section which consists of several parasequences composed of a basal, high API gamma-ray response CS overlain by a lower API response (Paxton et al., 2006) (Fig. 7). This stratigraphy was correlated to a subsurface well by Paxton et al. (Paxton et al., 2006) (Fig. 7), however, they place TSE's at the tops of the CS's, whereas we consider the base of the CS's to be TSE's. A similar sequence stratigraphy has been interpreted at the Wyche Farm quarry (Fig. 7). In the deeper subsurface, downlapping HST clinoforms can sometimes be identified on seismic reflection records (Fig. 7). Also, seismic interval mapping can identify areas within a 3D seismic survey area which are relatively enriched or impoverished in TOC (Fig. 8). At a smaller stratigraphic scale, some intervals contain interbedded chert and fissile shale, giving rise to a very complex gamma-ray log pattern. The chert beds are composed mainly of

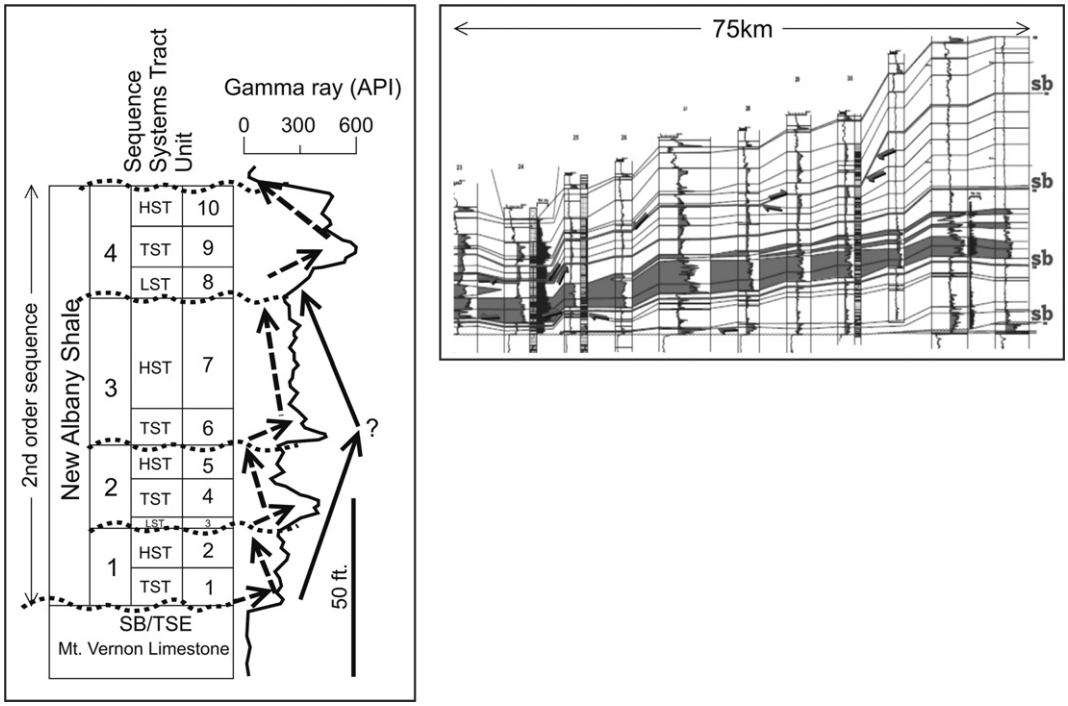

Fig. 6. 2nd and 3rd order sequence stratigraphy of the New Albany Shale, Illinois Basin, U.S.A. (Bohacs, 2010). The 2nd order sequence comprising the entire New Albany Shale sits atop a SB/TSE and consists of 4, 3rd order sequences (labeled 1–4). Only the uppermost sequence contains LST, so probably the other three 3rd order sequences sit upon TSE's. Solid and dashed arrows are explained in the caption of Fig. 3.

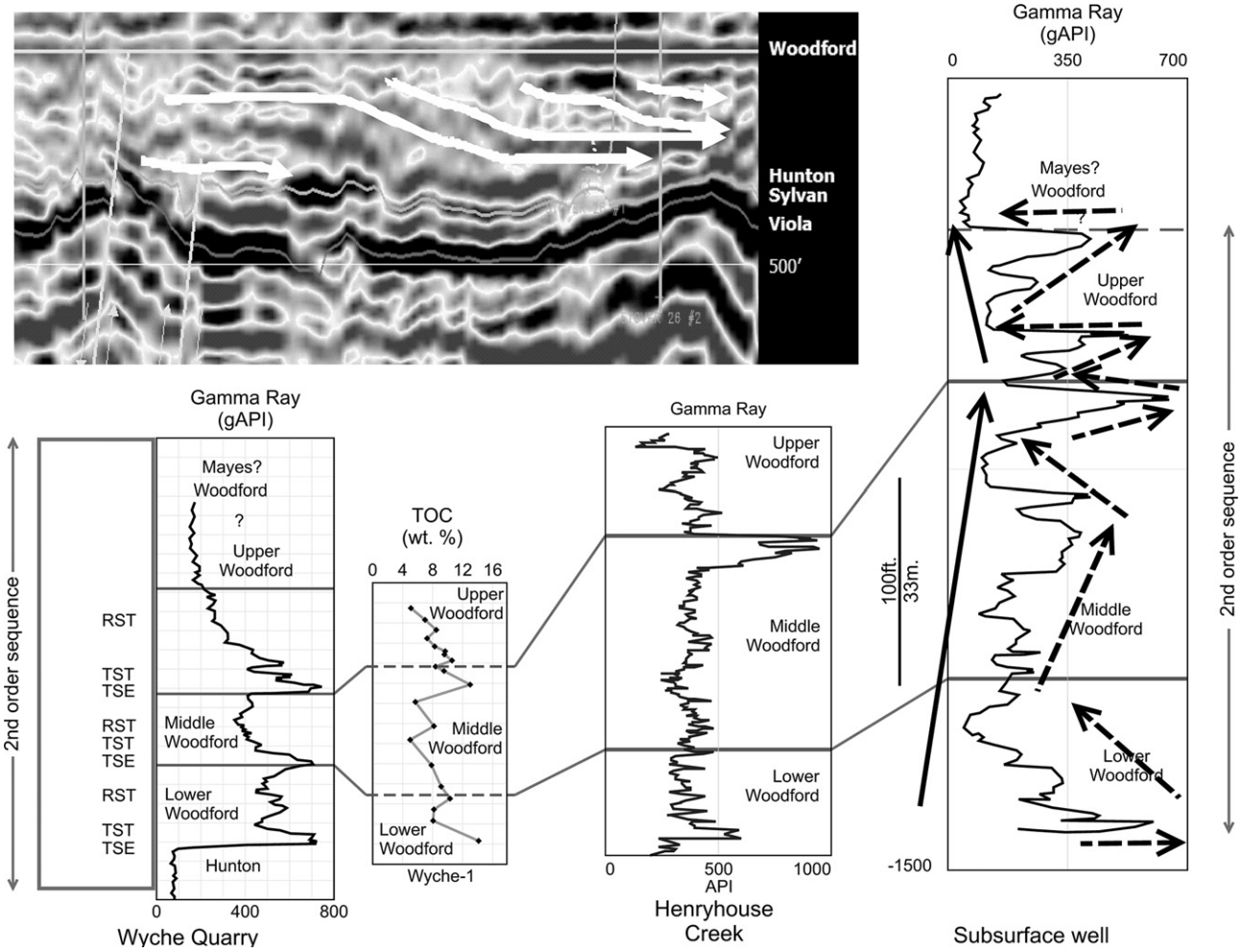

Fig. 7. Gamma-ray, TOC profile and sequence stratigraphy of the Woodford Shale from the Wyche Quarry, Oklahoma (modified from (Slatt et al., in press-b)) and the Henryhouse Creek outcrop (Paxton et al., 2006), correlated with a nearby subsurface well. TOC values are from a Wyche Quarry core. The Woodford is a 2nd order sequence with a number of higher frequency sequences superimposed. Solid and dashed arrows are explained in the caption of Fig. 3. Inset shows the downlap pattern of the 2nd order HST/RST onto the lowermost Woodford (after May and Anderson, 2010).

diagenetically-recrystallized radiolarians, providing a rigid, brittle framework, while the more ductile shale interbeds contain both detrital and authigenic quartz, clay (mainly illite), feldspar and >10 wt.% TOC (amorphous organic matter and *Tasmanites* cysts) (Fishman et al., 2010). Fractures are commonly at right angles to bedding within the brittle cherts, and either end abruptly at boundaries with the more ductile shale beds or they exhibit low angle shear planes (Badra, 2011). Woodford strata tend to be thicker in paleotopographic lows (probable incised valleys) upon the SB/TSE; this fact, coupled with the basal Woodford often being organic-rich (Fig. 7), provides an opportunity for localized accumulation of gas-prone facies.

3.5. The upper Mississippian ***Fayetteville Shale*** was deposited on a southward-deepening ramp in the eastern Arkoma Basin of Arkansas, USA prior to tectonic evolution of a foreland basin (Handford, 1986; Ratchford and Bridges, 2006). It generally becomes more clastic-poor and carbonate-rich upward from its base, and grades into the overlying Pitkin Limestone, indicating a 'deep shelf' (40–70 m) to shoreface depositional environment (Handford, 1986). High API gamma-ray, organic-pyritic shales, with some interbedded cherts, comprise the lower half of the Fayetteville (Fig. 9A), which is the most hydrocarbon-productive. The Fayetteville is underlain by the Boone Formation (limestone and chert), Batesville Formation (sandstone), and Moorefield Formation (shale) (Ratchford and Bridges, 2006). To our knowledge, no sequence stratigraphic interpretation has been published, however, the well log pattern (Fig. 9A) is typical of the other shales discussed in this paper.

3.6. The upper Misissippian ***Caney Shale*** occurs in the Arkoma and Ardmore basins of southern Oklahoma, USA along trend with the age-equivalent Fayetteville Shale in Arkansas (Andrews, 2007). The Caney generally consists of a lower, fissile shale interval and an upper shale-siltstone interval in the Arkoma Basin, but in the adjacent Ardmore Basin, the upper Caney contains limy interbeds with the shales (Fig. 9B). The Caney sits on either the Sycamore (also called Mayes) limestone-shale assemblage, or where absent, it sits unconformably (SB/TSE) on either the Woodford Shale or Hunton Limestone. The lower Caney is characterized by a high API gamma-ray log response atop the unconformity, a middle interval of lower gamma-ray response and an upper interval of variable API (Fig. 9B). The upper Caney is considered the primary gas-prone interval. To our knowledge, no sequence stratigraphic interpretation has been published, however, the well log pattern (Fig. 9B) is typical of the other shales discussed in this paper.

3.7. The middle–late Devonian ***Horn River Shale*** was deposited in the western Canada sedimentary basin (McPhail et al., 2009).

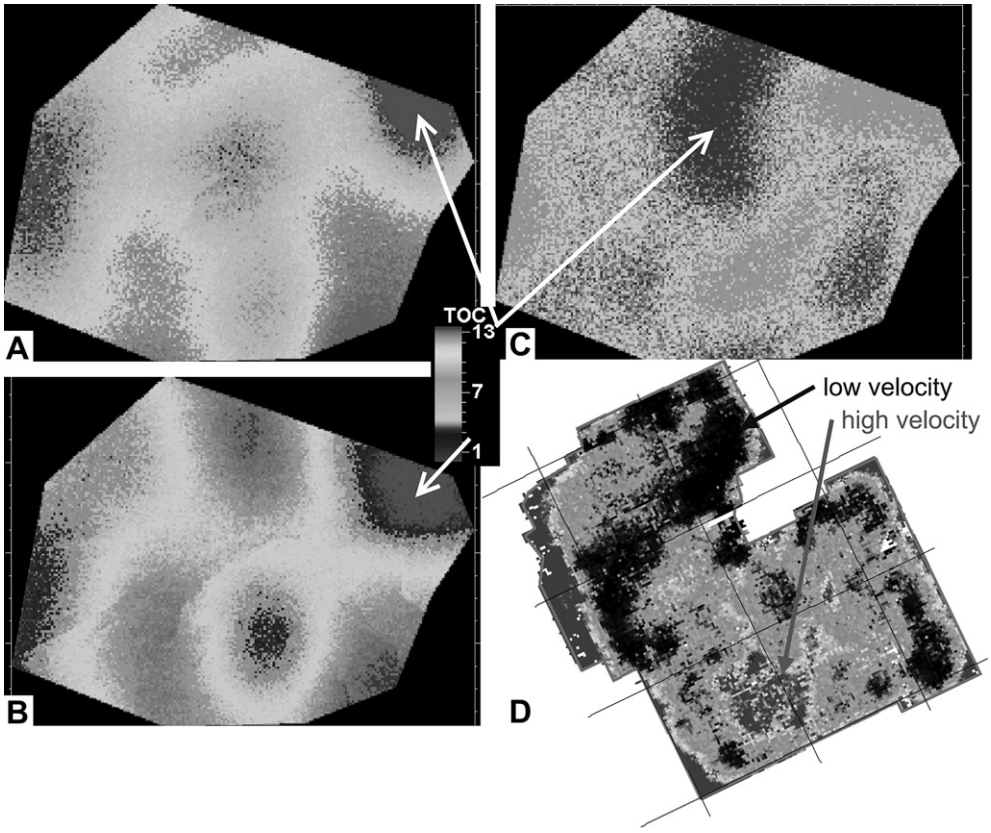

Fig. 8. A–C show log-derived TOC for three intervals within the Woodford Shale over a 15 km (6mi) area; A is top and C is bottom interval. TOC scale is from 1 to 13 wt. %. TOC for several wells were calculated from the sonic and resistivity logs using Passey et al., (Passey et al., 1990) method. D shows a seismic velocity distribution map of the Woodford based upon 3D seismic inversion; low velocity areas are dark and high velocity areas are light colored. There is a close correspondence between areas of high TOC and those of low seismic velocity and vice versa. This is an expected relation because the presence of lightweight TOC in a shale will reduce its density and sonic velocity, and its acoustic impedance.

From the base upward, it consists of the Evie member, which sits upon a Keg River limestone SB/TSE, then the Mid-Devonian 'Carbonate Member' (MDC), then the Otter Park member and at the top, the Muskwa member (Fig. 10). Both the Evie and the Muskwa members exhibit high API gamma-ray responses owing to their relative organic richness. The Evie member consists of gray–black, organic-rich, pyritic, sometimes calcareous, siliceous shale thus giving it the relatively high gamma-ray log response. The Otter Park member consists of gray calcareous shale. The Muskwa member is compositionally similar to the Evie member and also exhibits a high gamma-ray log response; it is gradational into the overlying Fort Simpson Formation. The Horn River Shale has been interpreted as consisting of two 2nd order depositional sequences—the lowermost being the Evie and the uppermost being the MDC–Otter Park–lower Muskwa (Hulsey, 2011). A 3rd order sequence stratigraphic framework is superimposed upon the 2nd order sequences (Fig. 10). TOC values generally track API gamma-ray values (Fig. 10). A 75 km long three-well cross section of the Muskwa member suggests a southward thinning and downlap onto a mfs, further supporting the 2nd order HST interpretation for the Muskwa (Fig. 11) (Hulsey, 2011).

3.8. The early Triassic ***Montney Shale*** was deposited in the western Canada sedimentary basin during marine transgression. It sits unconformably (SB/TSE) upon the Permo-Carboniferous Belloy/Debolt formations. The Montney is divided into two major 3rd order depositional sequences separated by a sequence boundary that correlates to an early Triassic global eustatic sea level fall (Moslow and Davies, 1997) (Fig. 12). The lower Montney consists of dark gray dolomitic siltstone interbedded with shales; it comprises a 3rd order TST and HST(RST), which are further subdivided into a series of 4th or 5th order progradational parasequences (shown by dashed arrows in Fig. 12) (Moslow and Davies, 1997). The upper Montney consists of siltstone with interlaminated fine-grained sandstones; it comprises LST turbidites (which form reservoirs in part of the basin) and a 3rd order TST/HST(RST) which also is divided into a number of progradational parasequences (dashed arrows in Fig. 12).

3.9. The Late Jurassic ***Haynseville and Bossier shales*** were deposited over a 15 My (140–155 My) time span in the East Texas and North Louisiana salt basins during opening of the Gulf of Mexico (Hammes and Carr, 2009; Hammes and Hamlin, 2010; Henk et al., 2010). The Haynseville (sometimes referred to as the lower Bossier) comprises a 2nd order TST unconformably (SB/TSE) overlying the Smackover/Haynesville Limestone (Fig. 13). The overlying Bossier Shale is interpreted as the 2nd order progradational HST(RST) of this system. Three main lithofacies comprise the Haynesville: siliceous mudstone, laminated calcareous mudstone, and calcareous bioturbated mudstone. Siliceous mudstone is more common in the northwest part of the Haynseville play area, and calcareous mudstone is more abundant to the southeast. Studies by Goldhammer (Goldhammer et al., 1999), Hammes and Hamlin (Hammes and Hamlin, 2010) and Henk et al. (Henk et al., 2010) have revealed a number of 3rd order sequences superimposed upon the 2nd order systems tracts, each being comprised of a lower, organic-rich TST and an upper calcareous mudstone HST(RST)

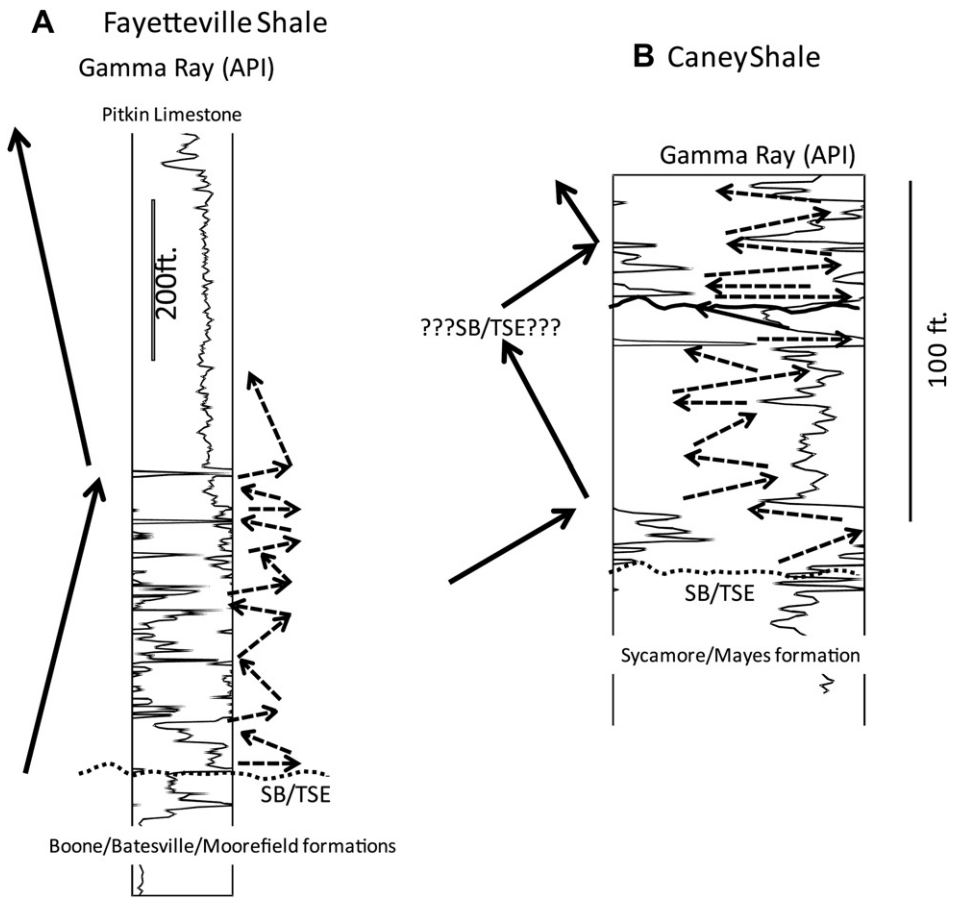

Fig. 9. (A) Gamma-ray profile of the Fayetteville Shale, Arkansas (modified from Ratchford and Bridges, 2006). (B). Gamma-ray profile of the Caney Shale in Oklahoma (modified from Andrews, 2007). Solid and dashed arrows are explained in the caption of Fig. 3.

(including low API gamma-ray/high density diagenetic dolomite marker beds) (Fig. 13). The basal 2nd order Haynesville TST is more organic-rich (up to 7 wt. %) than the Bossier HST (RST), making it a more prolific oil and gas producer.

3.10. The middle–upper Cretaceous (Cenomanian–Turonian) ***Eagle Ford Shale*** was deposited during the time interval 96–89 My ago in a drowned shelf setting in the East Texas basin, USA. It is part of a series of 2nd order 'supersequences' comprising Jurassic–Cretaceous Gulf Coast strata (Goldhammer et al., 1999). The organically-rich, lower Eagle Ford (i.e. Britton/Pepper Shale) sits atop the Buda Limestone erosional surface (SB/TSE), and is separated from the more calcareous upper Eagle Ford (i.e. Acadia Park) by a mfs dated at about 93.5 My (Cenomanian–Turonian boundary) (Treadgold et al., 2010) (Fig. 14B), thus the lower Eagle Ford is a 2nd order TST and the upper Eagle Ford is a 2nd order HST(RST). Depositional patterns are the result of interactions of basement zones of weakness, underlying carbonate paleogeography, salt tectonics, and eustatic sea level (Treadgold et al., 2010). The Eagle Ford is composed of a mix of platform-derived carbonate detritus from the Edwards/Stuart City trend and siliciclastics from the Woodbine delta. Overall, the Eagle Ford is locally calcite-rich, with lesser quartz and clays (illite–smectite) in the form of laminated, calcareous mudstone, burrowed calcareous mudstone, and burrowed lime mudstone/wackestone/packstone. The well-log patterns reflect these variations in facies, whereby the lower Eagle Ford TST exhibits an overall higher gamma-ray count than the upper Eagle Ford (Fig. 14B). A 60 m complete stratigraphic section from the top of the Buda Limestone to the top of the Eagle Ford Shale is superbly exposed at Lozier Canyon, Texas (Fig. 14A); an outcrop gamma-ray log of that section closely resembles that of the subsurface gamma-ray log shown in Fig. 14B (Donovan et al., 2011).

3.11. Upper (Maastrichtian) Cretaceous ***Lewis Shale*–Fox Hills Sandstone** was deposited in the Greater Green River Basin of Wyoming and Colorado, USA during a major marine transgression. Although to our knowledge it is not currently being seriously considered as a gas shale target, it exhibits characteristics similar to those of other active gas shale plays described above (Slatt et al., 2009). This well- studied shale (summarized in Slatt et al. (Slatt et al., 2009)) also has the advantage of sufficient biostratigraphic control to develop a 4th order sequence stratigraphic framework. Ammonite zonation indicates the Lewis Shale–Fox Hills Sandstone was deposited over a 1.9 My time interval (Fig. 15) (Pyles et al., 2009). The lower strata, deposited from 71.3 to 70.4 My comprises a 3rd order TST, which is overlain by a 70.4–69.4 My RST (Fig. 15). A regional cross section (Pyles et al., 2009) shows that the RST downlaps and progrades onto horizontally bedded strata capped by an organic-rich shale named the "Asquith Marker" (Fig. 16). The Asquith Marker is continuous across the entire Cretaceous Greater Green River Basin of the U.S. and is a 3rd order condensed section (Fig. 16). Several 4th order sequences of about 100,000–300,000 year duration are superimposed on the 3rd

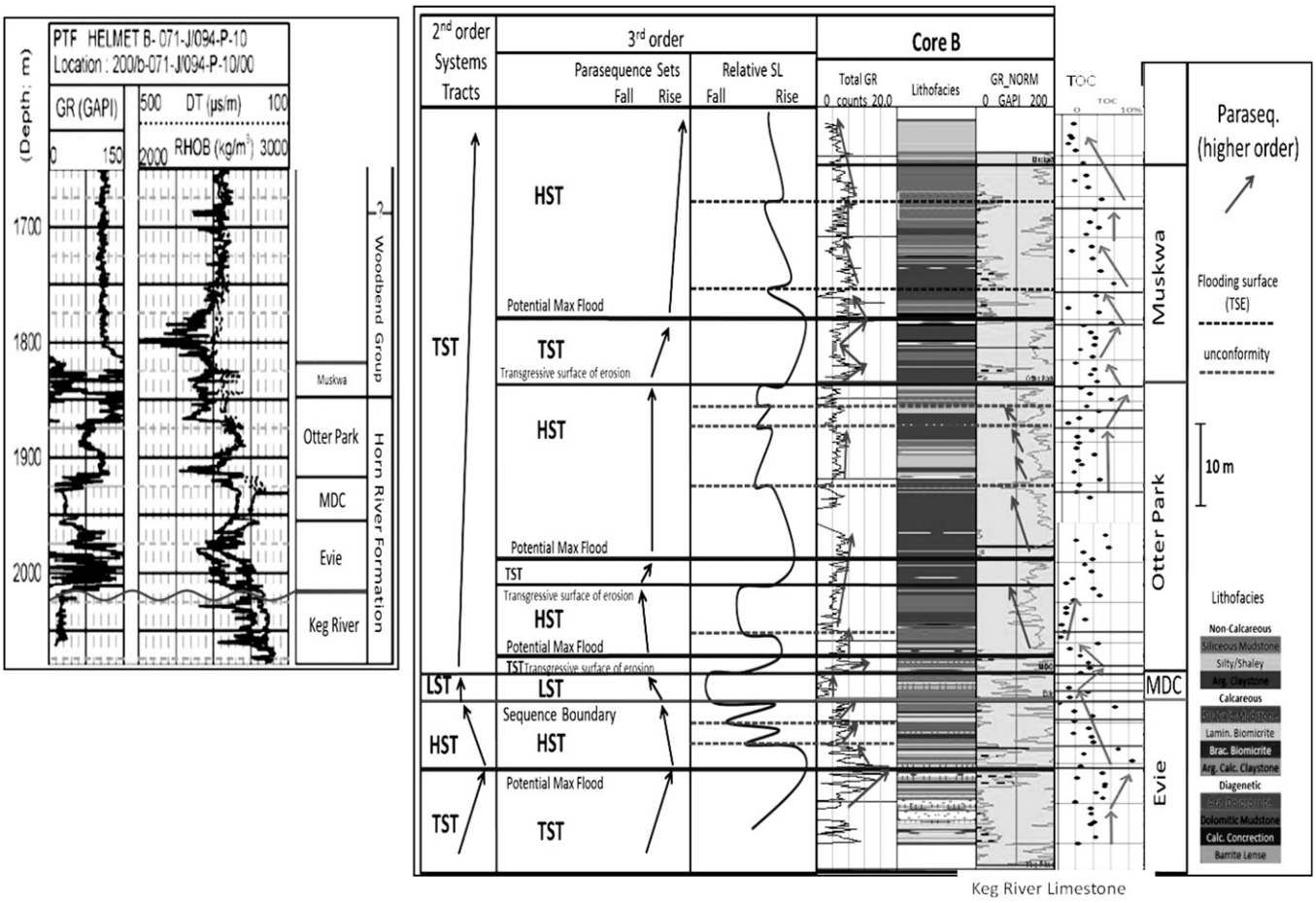

Fig. 10. Gamma-ray log showing the subdivision of the Horn River Shale into—from the base, upward—the Evie Shale, Middle Devonian Carbonate (MDC), Otter Park Shale and Muskwa Shale. 2nd and 3rd order sequences and systems tracts are shown along with an interpreted relative sea level curve. TOC trends track API gamma-ray log trends. Lithofacies are from description of Core "B". After Hulsey (2011).

order sequence (Figs. 15 and 16). In the part of the basin from which the well shown in Fig. 15 was drilled, most of the 4th order sequences contain LST gas-prone submarine fan sands overlain by shaly, and sometimes organic-rich TST/HST(RST) (Slatt et al., 2009)). Almond et al. (Almon et al., 2002) distinguished six shale facies within the Lewis on the basis of outcrop and well studies: (1) pyritic fissile shale (TOC 1–1.3 wt. %); (2) phosphatic shale (TOC 1.3–2.8 wt. %); (3) silty shale (TOC 1.1–1.5 wt. %); (4) silty calcareous shale (TOC 1.2–1.8 wt. %); (5) silty calcareous mudstone (TOC 0.6–0.7 wt. %); and (6) bioturbated argillaceous siltstone (0.5–0.6 wt. %). They interpreted Facies 1 as comprising TST, Facies 2 as 'condensed section' (a 3rd order condensed section termed the "Asquith Marker" is an areally extensive shale with local TOC's up to 12 + wt. %), and Facies 3–6 as HST(RST) (Almon et al., 2002). The main minerals comprising the shales are quartz and clays (illite, smectite, and chlorite).

3.12. The lower Silurian ***Longmaxi Shale*** was deposited in the Sichuan basin of southeast China. It is the largest gas-producing basin in China, with 700BCF produced from conventional strata in 2009 (Zheng, 2011). It is a highly carbonaceous (>4 wt. % TOC), sometimes silty shale that has tested gas and offers significant potential for shale gas. It is underlain by Ordovician carbonates. Although not as much is known of this potential resource, it is included in this paper mainly because gamma-ray logs (Fig. 17A) exhibit a similar 2-fold stratigraphic pattern to those shales discussed above.

3.13. The Upper Cretaceous ***Niobrara Formation*** was deposited along the broad, shallow eastern shelf of the Western Interior Seaway, USA. It is a carbonate-rich oil and gas play, so is presented in this paper for comparative purposes with the other shales. The Niobrara was deposited as a 3rd order sequence during a major marine transgression which encompassed a 6 My time span. May and Anderson (May and Anderson, 2010) identified alternating (cyclicial) chalk and marl intervals, with the chalks tending to have more carbonate and the marls tending to have more clay and quartz (Fig. 17B). Pollastro (Pollastro et al., 2007) subdivided the Niobrara components into (1) 'carbonate', which is mainly biogenic calcite (coccoliths, rhabdoliths, foraminfera, inocerimids, and oyster shells) and (2) 'acid insoluble residue' which is mainly clays (illite–smectite), pyrite, zeolites and organic matter (TOC ranges up to 6 wt.%).

3.14. Stratigraphic similarities and differences

The following geologic characteristics are generally common to the shales discussed above:

1. All the shales rest on an unconformity surface, which is interpreted as a combined sequence boundary (SB) formed during a drop in relative seal level, followed by further erosion during early transgression to give a transgressive surface of erosion (TSE).
2. High gamma-ray, normally organic-rich shales are TST's, or more specifically CS's that either sit directly on a TSE or cap

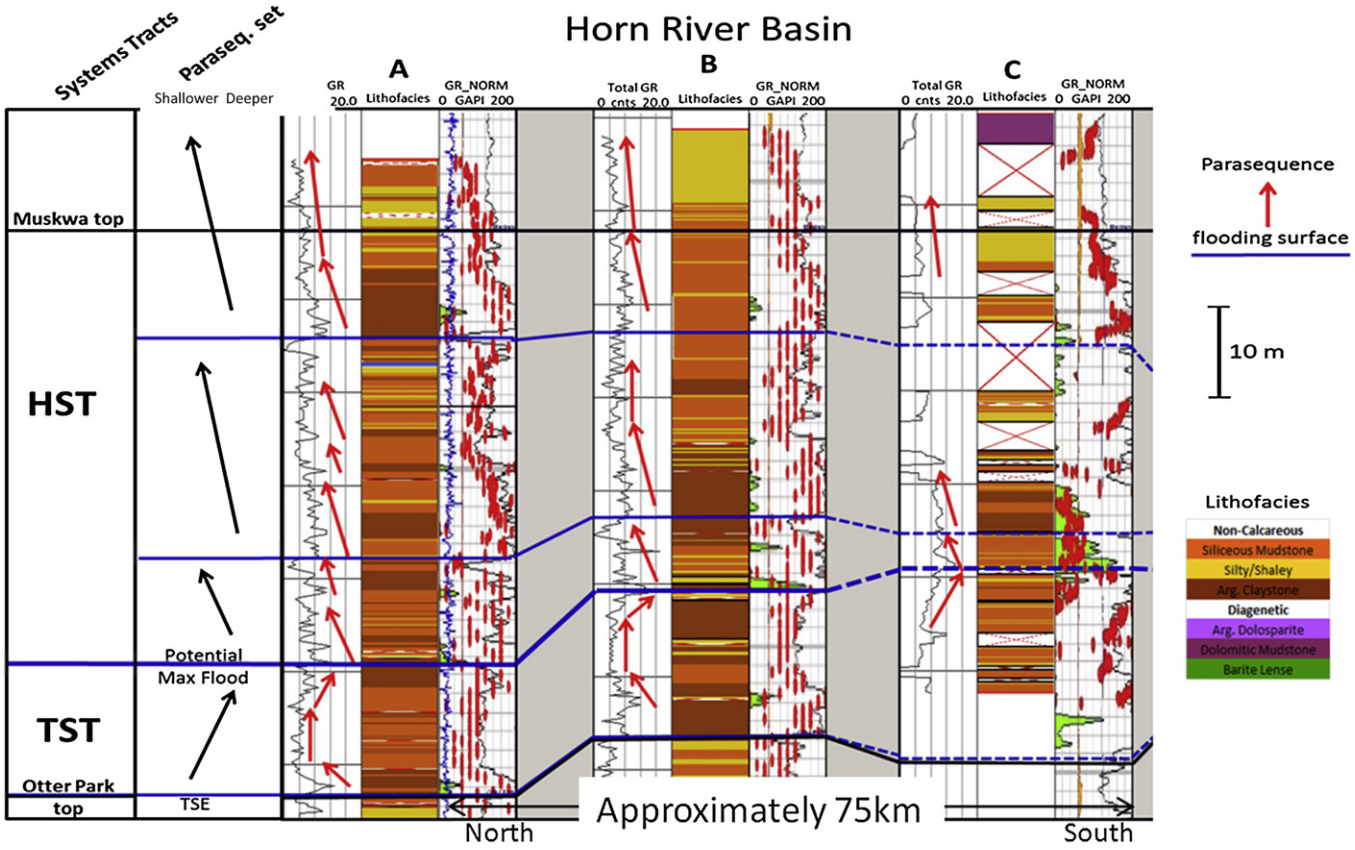

Fig. 11. 75 km long, 3 cored-well cross section of the Muskwa Interval of the Horn River Shale showing the 3rd order TST and HST, with higher frequency (4th order?) cycles superimposed. Approximate core locations are shown in the inset map. Note thinning of the HST toward the south onto the flooding surface, suggestive of southward progradation across the flooding surface. After (Hulsey, 2011).

a fining-upward trend above the TSE. The top of the high gamma-ray shale is a mfs.

3. Stratigraphically above the mfs are 'relatively cleaner' HST (RST) strata with a reduced API gamma-ray count.
4. The basic stratigraphy of TSE–TST, (CS)–HST(RST) occurs at 2nd, 3rd, and 4th order cyclicity where resolvable, giving rise to several high gamma-ray intervals within a shale stratigraphic sequence; such cyclicity in high and low API gamma-ray log response strata has been termed 'brittle-ductile couplets' by Slatt and Abousleiman (2011), who pointed out that sequence stratigraphy can be utilized as a tool for identifying and mapping zones with different geomechanical properties.
5. None of the gas shales discussed in this paper can be considered 'uniform black shales'. All exhibit varying degrees of stratification that can be related to eustatic/climatic controls on their depositional patterns.
6. Because of their organic richness, TST's, in particular their component CS's, have the highest potential gas content. When finely interbedded with more brittle rocks, such couplets contain both source and reservoir rock and have better potential to be hydraulically stimulated and produced.
7. The focus of this paper has been on vertical stratigraphy, with only a few examples of lateral variations within a stratigraphic sequence (Figs. 5–7, 11, 16). Those examples clearly demonstrate from log cross sections and seismic reflection profiles the common low-frequency sequence downlap of HST/RST strata onto a horizontal CS and mfs. Using this stratal pattern as a guideline, higher-frequency sequences can be laterally correlated and mapped for their contained organic-rich and organic-poor strata.
8. These features provide the basis for a unifying, general sequence stratigraphic model for shales that is based upon Exxon sequence stratigraphic concepts that are well-known and widely-used for sandstones and carbonates (Abreau et al., 2010). This model for shales provides the basis for predicting and mapping stratigraphy, and ultimately the most productive facies of unconventional gas shales.

The following attributes are generally not common to the shales discussed above.

1. Although the shales described above generally contain the same major components (quartz, carbonate, clays and organic matter) their proportions vary both vertically and laterally within each shale sequence as well as among the different shales; for example the Barnett is generally considered to be 'siliceous' while the Eagle Ford and Niobrara are generally considered to be 'calcareous' even though different stratigraphic intervals are compositionally diverse.
2. Detailed sequence stratigraphy has not been published, or perhaps even attempted for all of the shales described above.
3. Although identification of 2nd order sequence stratigraphic cyclicity can generally be biostratigraphially age-dated in Paleozoic shales, designation of higher frequency, datable cyclicity is more speculative owing to a lack of high frequency biostratigraphic resolution. In Mesozoic shales, biostratigraphic resolution may be sufficient to establish 3rd and 4th order cyclicity, as demonstrated for the Lewis Shale in this paper.

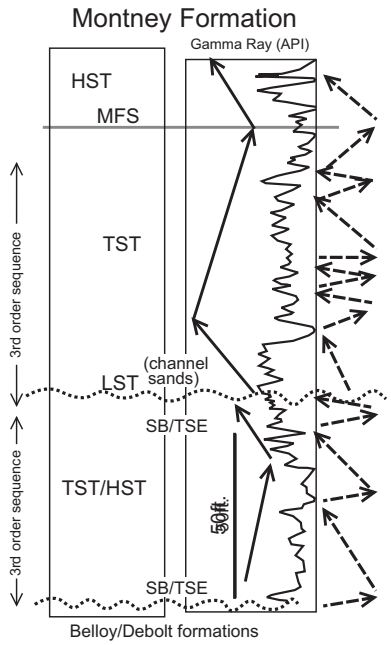

Fig. 12. Gamma-ray profile and 3rd order sequence stratigraphy of the Montney Formation, Canada (modified Moslow and Davies, 1997). Possible 4th order sequences are noted by the dashed arrows. Solid and dashed arrows are explained in the caption of Fig. 3.

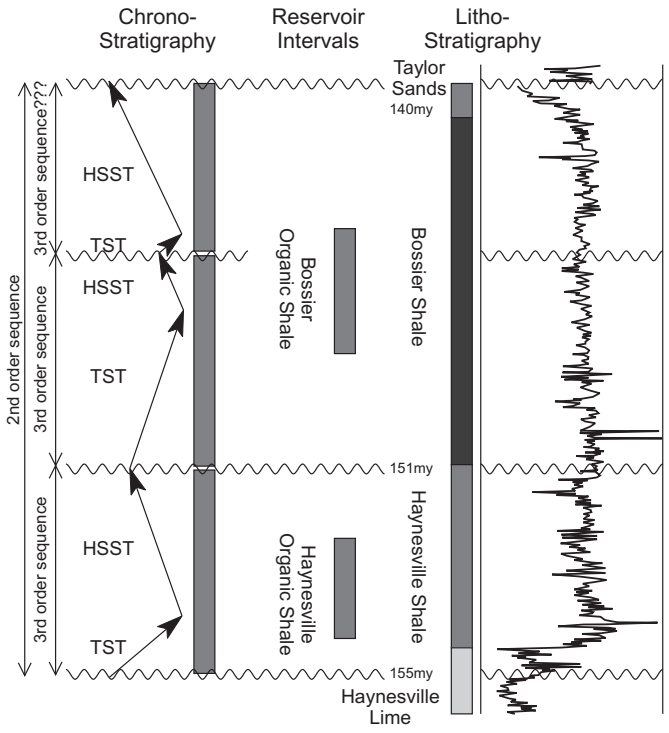

Fig. 13. Gamma-ray profile and 2nd and 3rd order sequence stratigraphy of the Haynesville/Bossier Shale, Texas and Lousiana, U.S.A. (modified from Hammes and Carr, 2009; Vorce, 2011). A 151 My sequence boundary separates the older Haynesville from the younger Bossier shale. Figure modified from (Vorce, 2011).

4. Comparative geochemistry

Conventional geochemical characterization of potential source rocks includes assessment of the rock's organic richness (i.e. total organic carbon-TOC) and quality (e.g. visual kerogen analysis, hydrogen index-HI) and maturity (e.g. T_{max}, vitrinite reflectance, etc) to estimate quantity and type of generated hydrocarbons. Oil-prone source rocks are traditionally defined as rocks characterized by TOC > 1% and HI > 350 mg HC/gm, while gas-prone source rocks are characterized by TOC > 0.5% and HI > 150 mg HC/gm (Hunt, 1996). Additionally, maturity windows calibrated against different

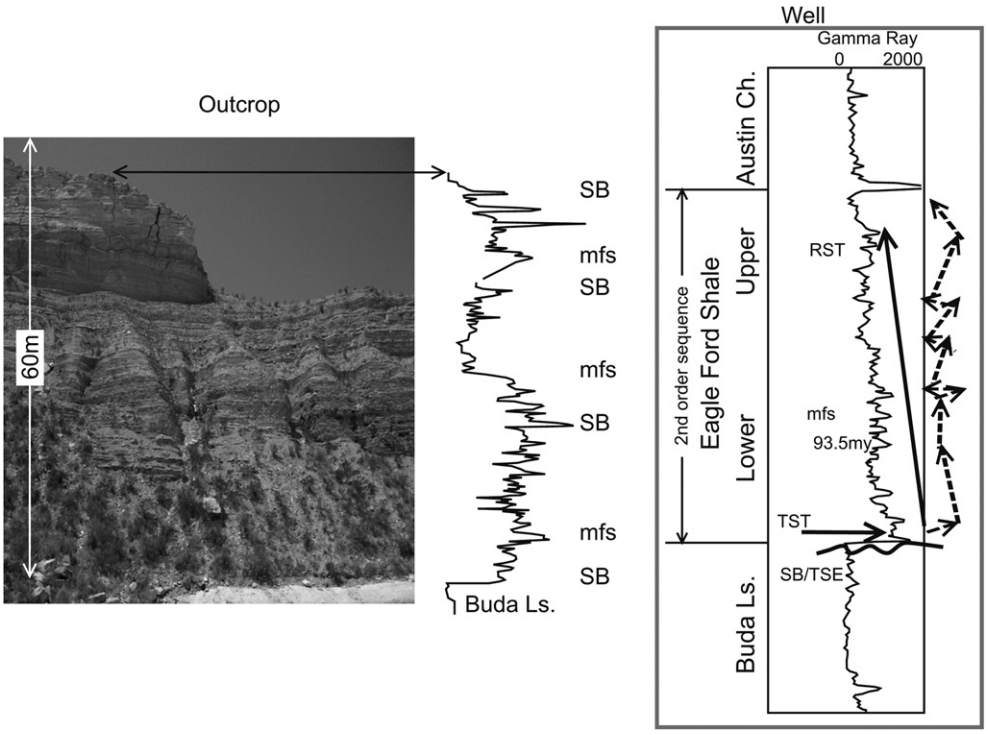

Fig. 14. Outcrop and subsurface well log gamma-ray profiles and 2nd order sequence stratigraphy of the Eagle Ford Shale, Texas (modified from Treadgold et al., 2010; Donovan et al., 2011). The photo on the left is of the complete Eagle Ford section at Lozier Canyon, south Texas, U.S.A. Solid and dashed arrows are explained in the caption of Fig. 3.

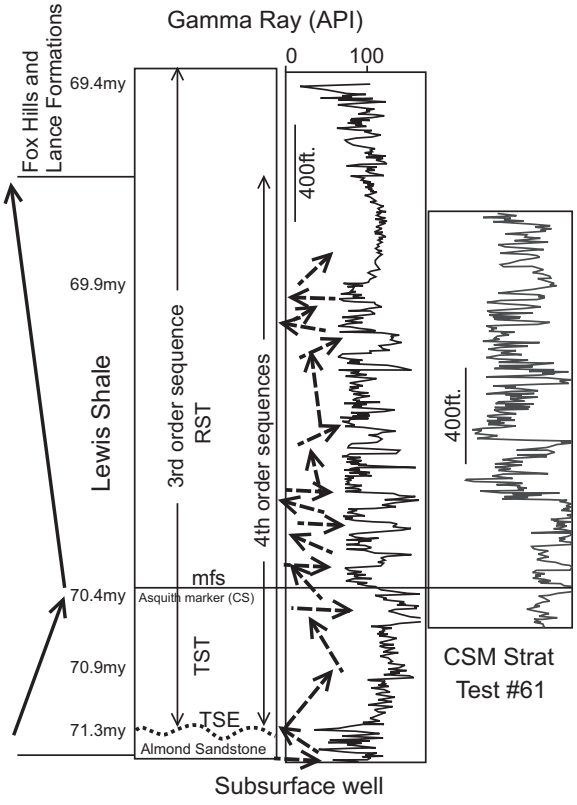

Fig. 15. Gamma-ray profile and 3rd and 4th order sequence stratigraphy of the Lewis Shale, Wyoming from a subsurface well and from a behind-outcrop shallow well (CSM Strat. Test #61) (Modified from Slatt et al., 2009). Solid and dashed arrows are explained in the caption of Fig. 3.

measurable parameters predict the main type of hydrocarbons that can be expected during each stage (e.g. oil and gas generation windows).

Comparison of geochemical characteristics of unconventional systems, however, has revealed a differing set of characteristics common to shale gas plays, but unlike the traditional definition of conventional gas-prone source rocks. These characteristics are discussed below.

4.1. Organic richness and type. Prolific gas-shale systems are usually characterized by high organic richness (usually greater than 3% TOC) (examples are provided in Figs. 3, 7 and 10) and HI values greater than 350 mg HC/g. These values are greater than the threshold values typical of gas generation from conventional gas-prone source rocks and similar to characteristics typical of type II kerogen-rich, oil-prone source rocks. TOC values generally track API gamma-ray log values. Visual kerogen analyses of several gas shales indicate a predominance of type II kerogen. Amorphous organic matter content of up to 93% and H/C ratio of 1.41 have been reported for the Barnett shale (Hill et al., 2007). Likewise, values of up to 80% amorphous kerogen and atomic H/C ratios ranging from 1.14 to 1.21 were reported by Lewan (Lewan, 1987) for immature Woodford shale samples.

4.2. Minerals as indicators of anoxic and oxic depositional environmental conditions. Some minerals which are indicators of marine depositional environments have been identified. Phosphatic nodules are usually present within organic rich intervals in the Barnett (Singh, 2008), Woodford (Buckner et al., 2009) and Montney (Adams, 2009) shales. These are usually interpreted as characteristic of transgressive conditions during deposition. Reducing conditions are also proposed as characteristic of the environments of deposition of gas shale systems. Presence of pyrite has been reported in Barnett (Singh, 2008), Haynesville (Hammes and Carr, 2009), Marcellus (Nyahay et al., 2007), Woodford (Buckner et al., 2009) and Horn River (McPhail et al., 2009) shales, attesting to reducing conditions. Pyrite dissemination in discrete intervals indicates that anoxic conditions were not persistent throughout shale deposition.

4.3. Relative hydrocarbon potential (RHP) as an Indicator of anoxic and oxic depositional environmental conditions. Fluctuations in oxygenation conditions are reflected by variations in the relative hydrocarbon potential ratio (RHP, S1 + S2/TOC). Slatt et al. (Slatt et al., in press-a) and Miceli-Romero (Miceli-Romero, 2010) noted stratigraphic variations in the RHP in the Barnett and Woodford shales respectively. In both cases, it was observed that changes in oxygen levels as indicated by the RHP showed a good correlation with changes in relative sea level fluctuations derived from the stratigraphic interpretations (Fig. 18 is an example from the

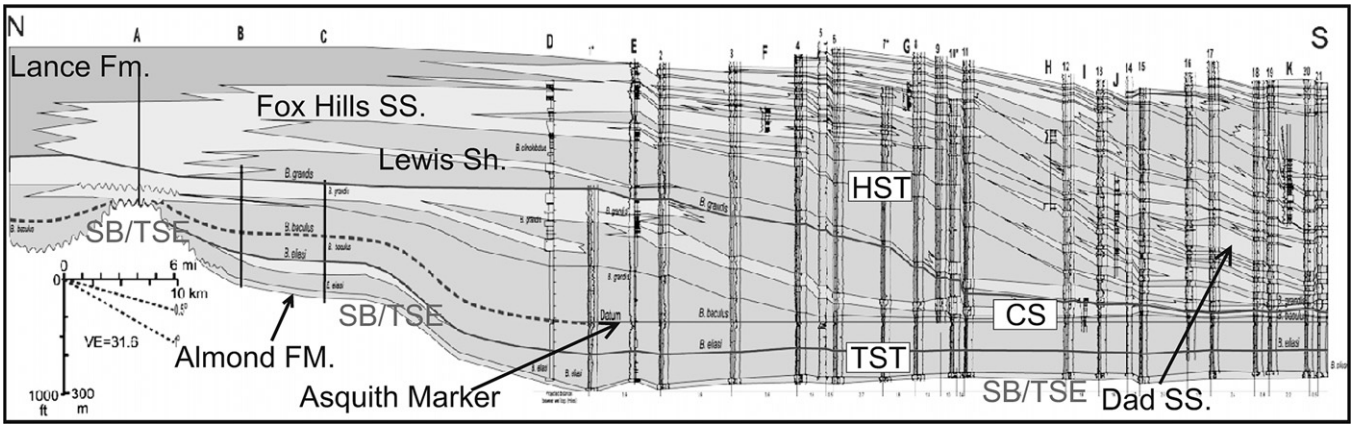

Fig. 16. North–South regional cross section of the Lewis Shale in Wyoming, U.S.A. The lower Lewis Shale is composed of a 3rd order transgressive systems tract (TST) sitting upon an unconformity (SB/TSE). The "Asquith Marker" is a 3rd order, organic-rich condensed section which extends across the entire Greater Green River basin and caps the TST. A 3rd order highstand systems tract (TST) downlaps onto the Asquith Marker. Several 4th order sequences, deposited over time intervals of 100,000–300,000 years, comprise the 3rd order HST. The downlapping 4th order boundaries were correlated across the area on the basis of ammonite zonations, volcanic ash horizons and organic-rich shales. The entire sequence was deposited over a 1.9 My (3rd order) time frame. The Dad Sandstone in this area is a series of gas-bearing slope and base-of-slope turbidite sandstones. (Modified from Pyles et al., 2009).

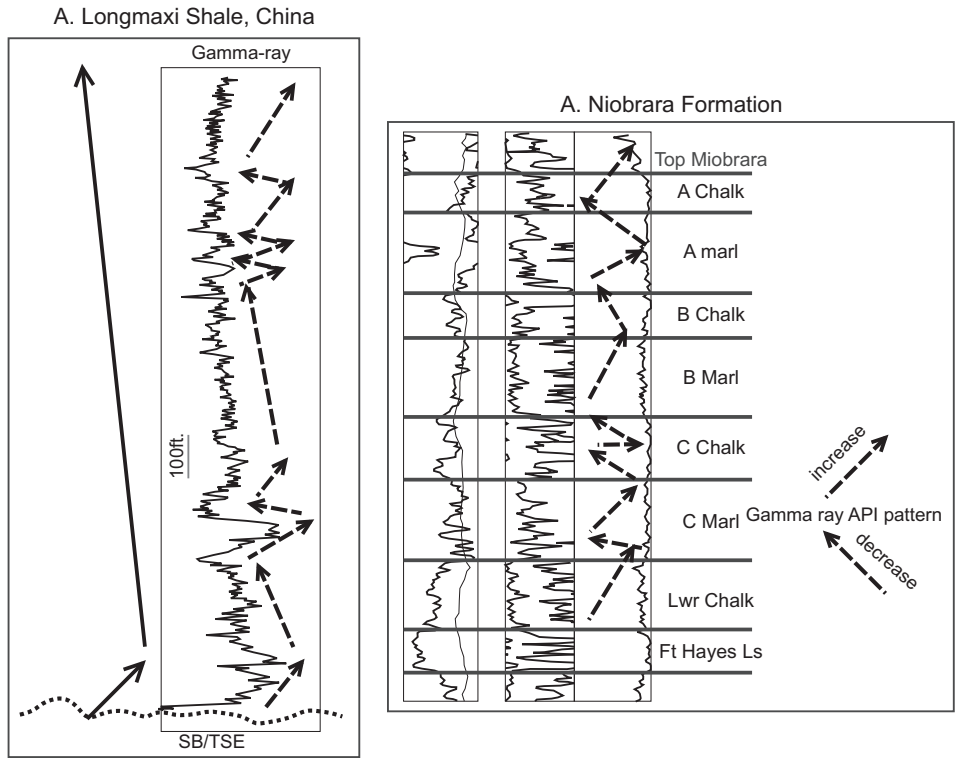

Fig. 17. A.Gamma-ray profile of the Silurian Longmaxi Shale, China. Solid and dashed arrows are explained in the caption of Fig. 3, and represent a hypothesized two-scale sequence stratigraphy based upon similarities with other shales discussed in this paper. B. Gamma-ray profile of the Niobrara Formation showing alternating Marl and Chalk strata and corresponding variations in gamma-ray pattern (modified from May and Anderson, 2010).

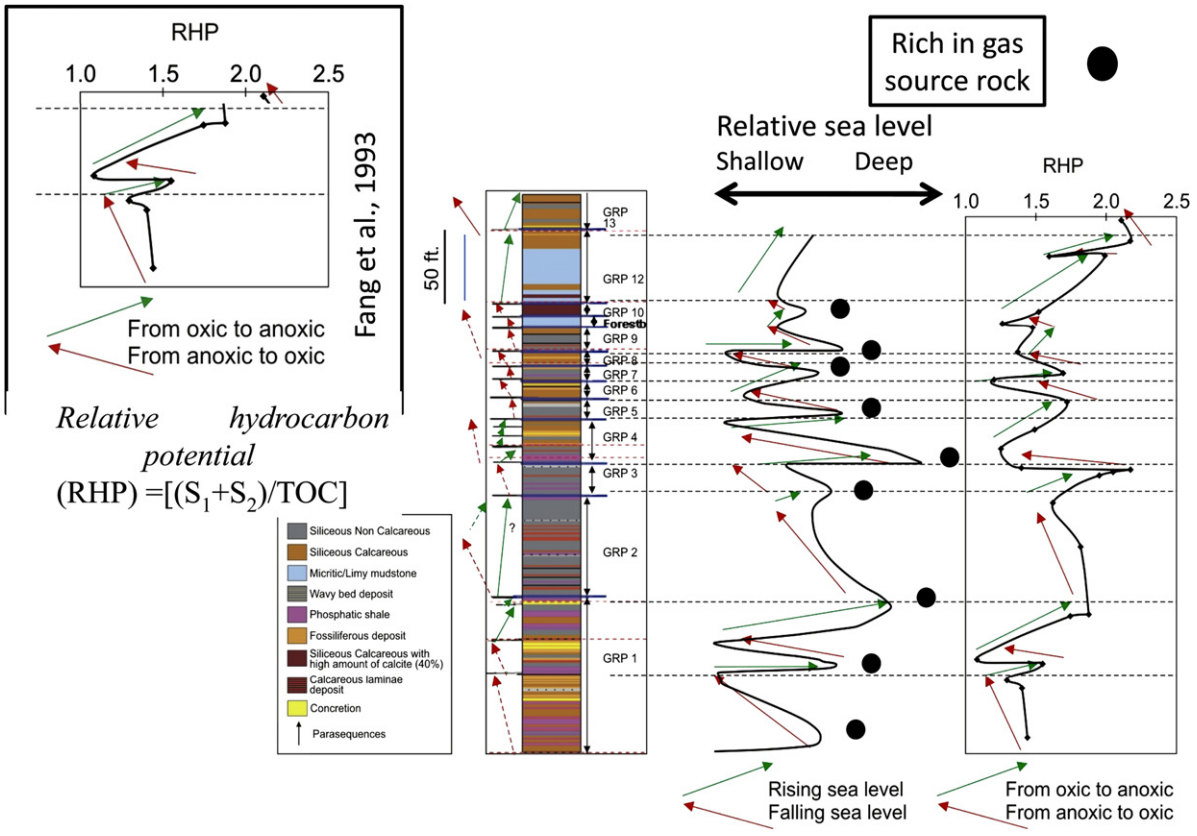

Fig. 18. Comparison of relative sea level and RHP curves for the Barnett Shale. Changes in oxic conditions as indicated by the RHP show a positive correlation with fluctuations in relative sea level, interpreted from lithofacies stacking patterns (Singh, 2008). (Modified from Slatt et al., in press-a; Miceli-Romero, 2010).

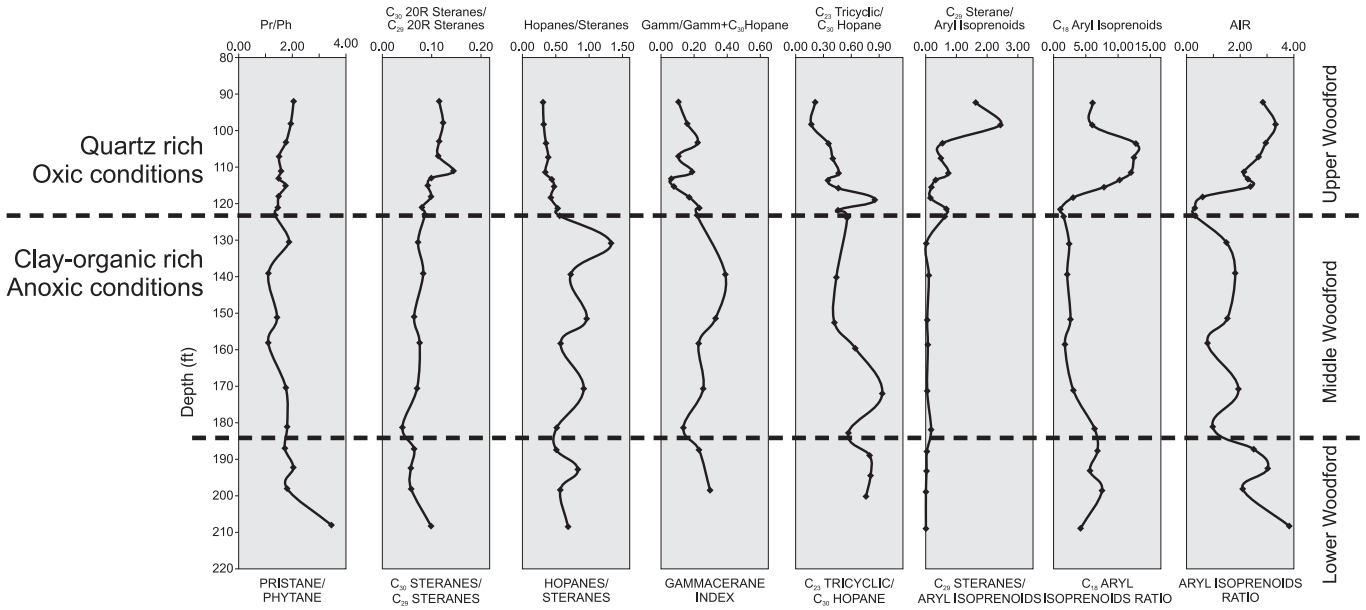

Fig. 19. Stratigraphic variations in various biomarker ratios for the Woodford Shale in the Wyche Quarry, Oklahoma (see Fig. 7 for comparison with gamma-ray log) (Miceli-Romero, 2010).

Barnett Shale). Depositional water depths with maximum RHP values (anoxic conditions) correspond with interpreted flooding surfaces, while minimum RHP values (oxic conditions) correlate with the location of sequence and parasequence boundaries.

4.4. Biomarkers as Indicators of anoxic and oxic depositional environmental conditions. Biomarker analyses are also in agreement with the hypothesis of fluctuating oxic conditions during deposition of gas shales. Rodriguez (Rodriguez, 2007) suggested that variations in the pristane/phytane ratio (Pr/Ph) and C_{13}–C_{20} regular isoprenoids measured in core extracts are associated with changes in redox conditions as well as variations in terrigenous input during deposition of the Barnett Shale. Similarly Miceli-Romero (Miceli-Romero, 2010) differentiated the upper and middle Woodford members based on the distribution of several biomarker ratios: pristane/phytane, hopanes/steranes, C_{23} tricyclic/C_{30} hopane, and C_{18} aryl isoprenoids (Fig. 19). More oxic conditions prevailed during deposition of the 'cleaner, organic-poor' upper Woodford as indicated by higher concentrations of C_{29} steranes. Dysaerobic to anaerobic environments prevailed during deposition of the middle Woodford shale as indicated by lower concentrations of Aryl isoprenoids derived from the green sulfur bacteria *Chlorobiaceae* (Fig. 19). Aryl isoprenoid ratios also indicated photic zone anoxia was episodic.

4.5. Thickness of organic-rich strata. Gross thickness of the organic-rich strata vary considerably, but are usually greater than 200 feet (65 m). Thicker source rocks have reduced expulsion efficiencies so that more hydrocarbons are retained during the initial stages of hydrocarbon generation, which are ultimately available for gas generation at later stages of source rock maturation. It is well recognized that at least a fraction of the hydrocarbons produced as part of the unconventional plays is the remaining hydrocarbons retained in the source rock after expulsion. For example, the Barnett is the main source rock of the conventional hydrocarbons present in the Fort Worth Basin, including the Pennsylvanian Boonsville conglomerate, Caddo Limestone and Strawn clastic reservoirs (Pollastro et al., 2007; Hill et al., 2007)) and the Woodford shale and its lateral equivalents have been geochemically correlated with oils produced in central and western Oklahoma (Comer and Hinch, 1987).

4.6. Organic maturity and isotopic composition. The main producing areas in shale-gas fields are usually delimited by organic maturity values greater than 1.1% Ro. By correlating isotopic and biomarker data with maturity measurements in the Barnett Shale, Rodriguez and Philp (Rodriguez and Philp, 2010) showed the Barnett shale reaches maturity values greater than 1.3% Ro in the main producing area. Moreover, in areas where maturity was predicted to be greater than 1.9%, Ro wetness reduction in gas composition and presence of an ethane isotope reversal were observed (Fig. 20). A reversal in the ratio of iC4/nC4 is also observed in samples with maturity values greater than 1.9% Ro. This isotope reversal has also been reported in other North American gas shales (Ferworn et al., 2008; Zumberge et al., 2009; Tilley et al., 2011) and is thought to be associated with secondary cracking of hydrocarbons.

Rodriguez and Philp (Rodriguez and Philp, 2010) used isotope analysis to illustrate how gases produced from the Barnett Shale were the product of secondary cracking of hydrocarbon. Hydrocarbons generated during the first stages of oil and gas generation are relatively depleted in ^{13}C compared to the original isotopic composition of the kerogen. Early generated hydrocarbons retained in the source rock after expulsion are cracked to gas at later stages of maturity, contributing ^{12}C to the gas being generated directly from the kerogen and causing the observed isotope reversal (Fig. 20).

It has also been proposed that wells were the isotope reversal has been observed are the best producers in gas-shale plays (Ferworn et al., 2008). Comparison of isotopic data and published normalized cumulative production in the Barnett Shale (Fig. 21) indicates this correlation exists at least in this prolific gas-shale play.

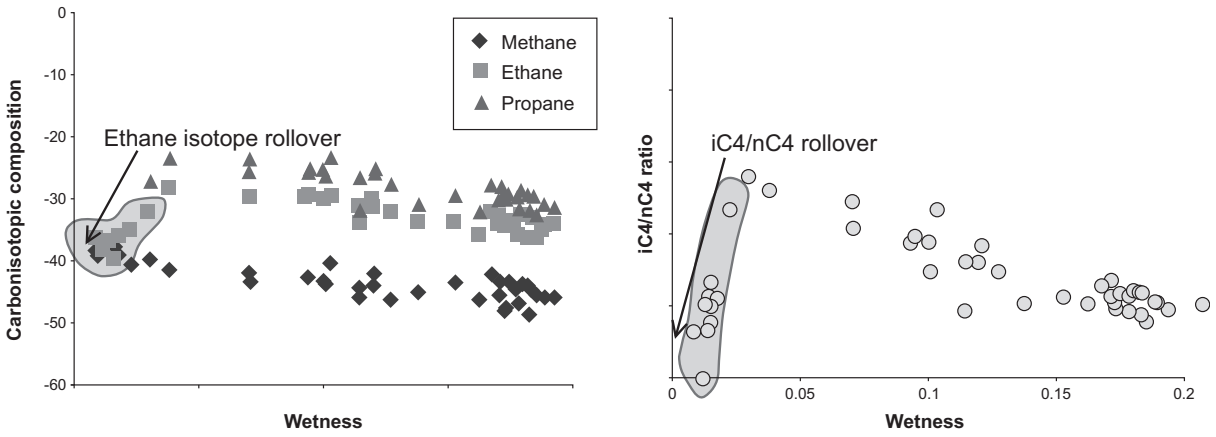

Fig. 20. The ethane isotope rollover from Barnett Shale samples with maturity values >1.9% Ro. The same rollover is observed in the ratio of iC4/nC4.

5. Conclusions: integrating sequence stratigraphy and geochemistry

Combining the stratigraphic and geochemical analyses of the gas-shales mentioned above has highlighted a series of common characteristics that can be grouped into a predictive model to explore for and develop gas-shale plays. This general model is shown in Fig. 22. Organic rich (TOC > 3%) intervals are those positioned as condensed sections (CS) (of various geological time scales) that sit atop a SB/TSE and directly beneath a mfs. Those with total thicknesses >200 ft.(65 m), with predominance of Type II kerogen that have reached maturity values >1.1% Ro have the greatest potential to become successful gas-shale plays. These features are mappable using sequence and seismic stratigraphic concepts and correlation strategies. In addition, zones where ethane isotope and iC4/nC4 ratio reversals have been observed seem to represent areas where increased gas producibility can be expected.

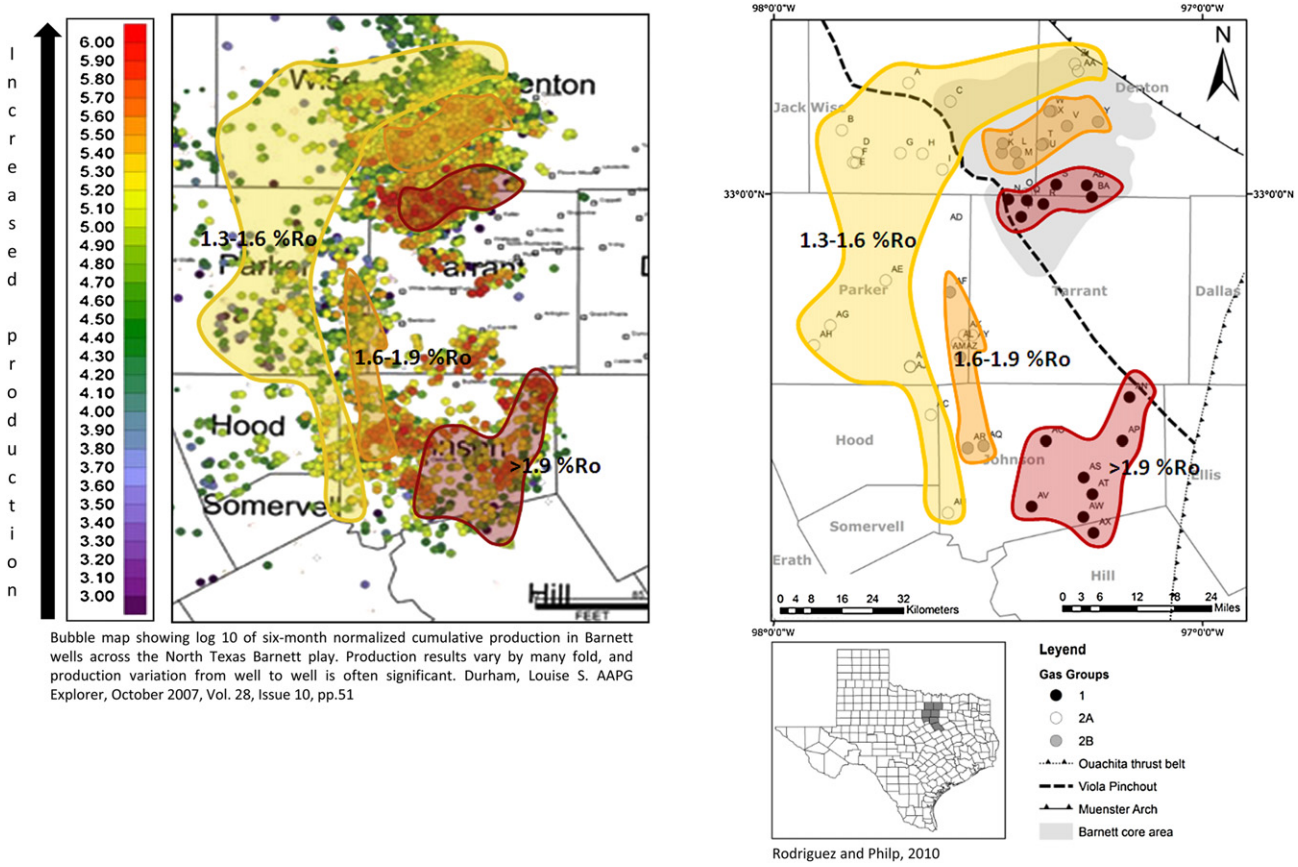

Bubble map showing log 10 of six-month normalized cumulative production in Barnett wells across the North Texas Barnett play. Production results vary by many fold, and production variation from well to well is often significant. Durham, Louise S. AAPG Explorer, October 2007, Vol. 28, Issue 10, pp.51

Rodriguez and Philp, 2010

Fig. 21. Higher maturity areas showing ethane isotope and iC4/nC4 ratio rollover correlation with higher production.

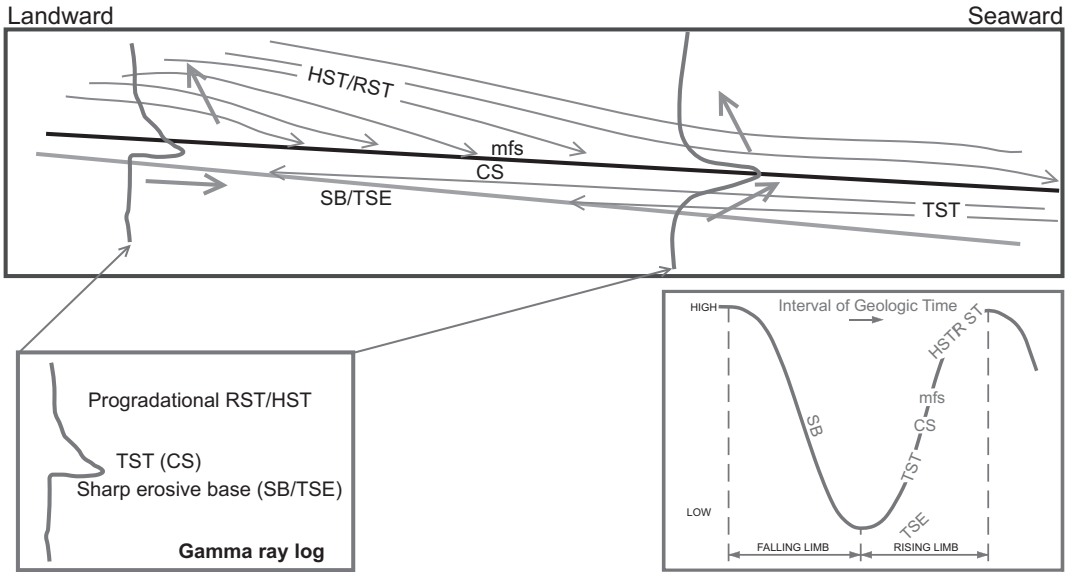

Fig. 22. General sequence stratigraphic model for gas shales. The shales sit upon a combined sequence boundary (SB-formed during falling stage of sea level) and transgressive surface of erosion (TSE-formed during early transgression). The lowermost transgressive marine shale is generally organic-rich, forming a relatively high gamma-ray condensed section (CS) atop the sequence boundary. The top of the CS is the maximum flooding surface (mfs) upon which highstand, progradational (regressive), less organic-rich strata of the highstand/regressive systems tract (HST/RST) downlap onto. The two hypothetical gamma-ray logs show the positions of the CS relative to the SB/TSE; hypothetically, the farther seaward the strata, the greater the stratigraphic thickness will be between the SB/TSE and the CS and mfs (assuming depositional occurred on a seaward-sloping surface). The relative sea level curve shows upon which part of the sea level cycle each feature will be formed.

Acknowledgments

We extend our thanks to Dr. Paul Philp for valuable advice during the course of this study, Andrew Slatt for providing many of the graphics, Dr. Barry Katz for valuable comments and suggestions during the reviewing process and Chevron Energy Technology Co. for allowing publication of the geochemistry part of this paper.

References

Abouelresh, M.O., Slatt, R.M., 2012. Lithofacies and High-frequency Sequence Stratigraphy of the Barnett Shale in the East-central Fort Worth Basin, American Association of Petroleum Geologists Bulletin, pp. 1–22.

Abreau, V., Neal, J.E., Bohacs, K.M., Kalbas, J.L., 2010. Sequence Stratigraphy of Siliciclastic Systems—The ExxonMobil Methodology. In: SEPM Concepts in Sedimentology and Paleontology, vol. #9, 226 pp.

Adams, C., 2009. Shale gas Activity in British Columbia, Exploration and Development of BC's shale gas areas. Ministry of energy, Mines and petroleum resources, resource Development and Geoscience Branch, 3rd Annual unconventional gas Technical Forum.

Almon, W.R., Dawson, W.C., Sutton, S.J., Ethridge, F.G., Castelblanco, B., 2002. Sequence stratigraphy, facies variation, and petrophysical properties in deepwater shales, Upper Cretaceous Lewis Shale, south-central Wyoming. Gulf Coast Association of Geological Society Transactions 52, 1041–1053.

Andrews, R.D., July-Aug., 2007. Stratigraphy, production, and reservoir characteristics of the Caney Shale in southern Oklahoma. Shale Shaker, 9–25.

Badra, H., 2011. Field characterization and analog modeling of natural fractures in the Woodford Shale, Southeast Oklahoma, unpubl. M.S. thesis, Univ. Oklahoma.

Bohacs, K., 2010. Sequence stratigraphy in fine-grained rocks at the field to flow-unit scale: insights for correlation, mapping and genetic controls, in Houston Geol. Soc. Applied Geoscience Conf of US Gulf Region Mudstones as unconventional shale gas/oil reservoirs, Feb. Houston, TX.

Bowker, K.A., Grace, T., 2010. The downside of using GR to determine TOC content: an example from the Marcellus Shale in SE West Virginia. In: Critical Assessment of Shale Resource Plays, AAPG Hedberg Research Conference, Dec., Austin, TX.

Boyce, M.L., Yanni, A.E., Carr, T.R., 2010. Depositional control of organic content in the middle Devonian Marcellus interval of West Virginia and western Pennsylvania. In: Critical Assessment of Shale Resource Plays, AAPG Hedberg Research Conference, Dec., Austin, TX.

Buckner, N., Slatt, R.M., Coffey, B., Davis, R.J., 2009. Stratigraphy of the Woodford Shale from Behind-outcrop Drilling, Logging, and Coring. AAPG Annual Convention, San Antonio, TX. AAPG Search and Discovery Article No. 50147. http://www.searchanddiscovery.net/documents/2009/50147buckner/ndx_buckner.pdf (accessed 19.04.10.).

Comer, J.B., Hinch, H.H., 1987. Recognizing and quantifying expulsion of oil from the Woodford Formation and age-equivalent rocks in Oklahoma and Arkansas. American Association of Petroleum Geologists Bulletin 71, 844–858.

Donovan, A.D., Staerker, T.S., Weiguo, L., Pramudito, A., Evenick, J., McClain, T., Agrawal, A., Banfield, L., Land, S., Corbett, M.J., Lowery, C.M., Miceli-Romero, A., 2011. Field guide to the Eagle Ford (Boquillas) formation: west Texas. American Association of Petroleum Geologists Field Seminar 144.

Ferworn, K.J., Zumberge, J., Reed, J., Brown, S., 2008. Gas Character Anomalies Found in Highly Productive Shale Gas Wells. http://www.papgrocks.org/ferworn_p.pdf (accessed 5.10.10.).

Fishman, N.S., Ellis, G.S., Paxton, S.T., Abbott, M.M., Boehlke, A.R., 2010. Gas storage in the upper Devonian–lower Mississippian Woodford Shale Arbuckle Mountains, Oklaoma—How much of a role do the cherts play?. In: Critical Assessment of shale resource plays, AAPG Hedberg Research Conference, Dec., Austin, TX.

Goldhammer, R.K., 1999. Mesozoic sequence stratigraphy and paleogeographic evolution of northeast Mexico. In: Bartolini, C., Wilson, J.L., Lawton, T.F. (Eds.), Mesozoic Sedimentary and Tectonic History of North-central Mexico. Geological Society of America Special Paper 340, pp. 1–58.

Hammes, U., Carr, D.L., 2009. Sequence Stratigraphy, Depositional Environments, and Production Fairways of the Haynesville Shale-Gas Play in East Texas, Search and Discovery Article #110084. http://www.searchanddiscovery.com/documents/2009/110084hammes/ndx_hammes.pdf (accessed 29.12.10.).

Hammes, U., Hamlin, S., 2010. New Insights into Facies, Depositional Environments, Sequence Stratiigraphy and Regional Extent of the Haynesville Shale of East Texas and Louisiana. In: Houston Geol. Soc. Applied Geoscience Conf of US Gulf Region Mudstones as Unconventional Shale Gas/oil Reservoirs, Feb. Houston, TX.

Handford, C.R., 1986. Facies and bedding sequences in shelf-storm deposited carbonates—Fayetteville Shale and Pitkin Limestone (Mississippian), Arkansas. Journal of Sedimentary Petrology 56, 123–137.

Henk, B., Sinclair, S., Juett, A., Bagley, J., Nicklin, D., King, S., 2010. The stratigraphic framework of the Haynesville shale in northwest Louisiana and northeast Texas. In: Critical Assessment of Shale Resource Plays, AAPG Hedberg Research Conference, Dec., Austin, TX.

Hill, R., Jarvie, D., Zumberge, J., Henry, M., Pollastro, R., 2007. Oil and gas geochemistry and petroleum systems of the Fort Worth Basin. American Association of Petroleum Geologists Bulletin 91, 445–473.

Hulsey, K.M., 2011. Lithofacies characterization and sequence stratigraphic framework for some gas-bearing shales within the Horn River Basin, northeastern British Columbia, unpubl.. M.S. Thesis, Univ. Oklahoma, 65.

Hunt, J.M., 1996. Petroleum Geochemistry and Geology. W.H. Freeman and Company, New York. 743.

Lash, G., Engelder, T., 2011. Thickness trends and sequence stratigraphy of the middle Devonian Marcellus formation, Appliachian basin: implications for Acadian foreland basin evolution. American Association of Petroleum Geologists Bulletin 95, 61–103.

Laughrey, C.D., Lemmens, H., Ruble, T.E., Butcher, A.R., Walker, G., Kostelnik, J., Barnes, J., Knowles, W., 2010. Black shale diagenesis: insights from integrated

high-definition analyses of post-mature Marcellus Formation rocks, northeastern Pennsylvania. In: Critical Assessment of Shale Resource Plays, AAPG Hedberg Research Conference, Dec., Austin, TX.

Lewan, M.D., 1987. Petrographic study of primary petroleum migration in the Woodford Shale and related rock units. In: Doligez,, B. (Ed.), Migration of Hydrocarbons in Sedimentary Basins. Editions Technip, Paris, pp. 113–130.

May, J.A., Anderson, D.S., 2010. Mudrock reservoir description and stratigraphy: not homogenous, not boring. In: Critical Assessment of Shale Resource Plays, AAPG Hedberg Research Conference, Dec., Austin, TX, 2010.

McPhail, S., Walsh, W., Lee, C., Monahan, P.A., 2009. Shale Units of the Horn River Formation, Horn River Basin and Cordova Embayment, Northeastern British Columbia. British Columbia Ministry of Energy, Mines and Petroleum Resources. http://www.empr.gov.bc.ca/OG/oilandgas/petroleumgeology/UnconventionalOilAndGas/Pages/Shale.aspx (accessed 18.04.10.).

Miceli-Romero, Andrea, 2010. Geochemical characterization of the Woodford Shale, central and southeastern Oklahoma. M.S. Thesis, The University of Oklahoma.

Moslow, T.F., Davies, G.R., 1997. Turbidite reservoir facies in the lower Triassic Montney Formation, west-central Alberta. Bulletin of Canadian Petrology Geology 45, 507–536.

Nyahay, R., Leone, J., Smith, L., Martin, J., Jarvie, D., 2007. Update on the Regional Assessment of Gas Potential in the Devonian Marcellus and Ordovician Utica Shale sin New York. Search and Discovery Article #10136. http://www.searchanddiscovery.net/documents/2007/07101nyahay/images/nyahay.pdf (accessed 18.04.10.).

Passey, Q.R., Creaney, S., Kulla, J.B., Moretti, F.J., Stroud, J.D., 1990. A practical model for organic richness from porosity and resistivity logs. American Association of Petroleum Geologists Bulletin 74, 1777–1794.

Paxton, S.T., Cruse, A.M., Krystyniak, A.M., 2006. Fingerprints of Global Sea-level Change Revealed in Upper Devonian/Lower Mississippian Woodford Shale of South-central Oklahoma. AAPG Search and Discovery Article #4021.

Pollastro, R.M., Jarvie, D.M., Hill, R.J., Adams, C.W., 2007. Geologic framework of the Mississippian Barnett shale, Barnett-Paleozoic total petroleum system, Bend arch-Fort Worth basin, Texas. American Association of Petroleum Geologists Bulletin 91, 405–436.

Pyles, D.R., Slatt, R.M., 2009. Stratigraphic evolution of the Upper Cretaceous Lewis Shale, southern Wyoming: applications to understanding shelf to base-of-slope changes in stratigraphic architecture of mud-dominated, progradational depositional systems. In: Nilsen, T., Shew, R., Steffens, G., Studlick, J. (Eds.), Atlas of Deepwater Outcrops, American Association of Petroleum Geologists Studies in Geology 56, pp. 485–489.

Ratchford, M.E., Bridges, L.C., 2006. Geochemistry and thermal maturity of the upper Mississippian Fayetteville shale formation, eastern Arkoma basin and Mississippi Embayment regions, Arkansas. Gulf Coast Association of Geological Societies Transactions 56, 717–722.

Rodriguez, N.D., Philp, R.P., 2010. Geochemical characterization of gases from the Mississippian Barnett shale, Forth Worth basin, Texas. American Association of Petroleum Geologists Bulletin 9411, 1641–1656.

Rodriguez, N., 2007. Geochemical characterization of gases from the Barnett shale, Forth Worth basin, Texas. M.S. Thesis, The University of Oklahoma.

Singh, P., 2008. Lithofacies and sequence stratigraphic framework of the Barnett Shale, northeast Texas. Unpubl.. Ph.D. Dissertation, The University of Oklahoma, 151.

Slatt, R.M., Abousleiman, Y., March, 2011. Merging sequence stratigraphy and geomechanics for unconventional gas shales. The Leading Edge, 274–282.

Slatt, R.M., O'Brien, N.R., 2011. Pore Types in the Barnett and Woodford Gas Shales: Contribution to Understanding Gas Storage and Migration Pathways in Fine-grained Rocks. American Association of Petroleum Geologists Bulletin, p. 2017 and 2030.t.

Slatt, R.M., Minken, J., Van Dyke, S.K., Pyles, D.R., Witten, A.J., Young, R.A., 2009. Scales of heterogeneity of an outcropping leveed-channel system, Cretaceous Dad sandstone member, Lewis shale, Wyoming, USA. In: Nilsen, T., Shew, R., Steffens, G., Studlick, J. (Eds.), Atlas of Deepwater Outcrops American Association of Petroleum Geologists Studies in Geology 56, pp. 490–496.

Slatt, R.M., Philp, R.P., O'Brien, N.R., Abousleiman, Y., Singh, P., Eslinger, E.V., Perez, R., Portas, A.R.M., Baruch, E., Marfurt, K.J., Madrid-Arroyo, S., Pore- to regional-scale, integrated workflow for unconventional gas shales. In: Breyer, J. (Ed.), Shale reservoirs: Giant resources for the 21st century AAPG Memoir 97, in press-a.

Slatt, R.M., Portas, A.R.M., Buckner, N., Abousleiman, Y., O'Brien, N., Tran, M., Sierra, R., Philp, P., Miceli-Romero, A., Davis, R., Wawrzyniec, T., Outcrop/Behind Outcrop (quarry) multiscale characterization of the Woodford gas shale, Oklahoma. In: Breyer, J., (Ed.), Shale reservoirs: Giant resources for the 21st century AAPG Memoir 97, in press-b.

Tilley, B., McLellan, S., Hiebert, S., Quartero, B., Veilleux, B., Muehlenbachs, K., 2011. Gas isotope reversals in fractured gas reservoirs of the western Canadian Foothills: mature shale gases in disguise. American Association of Petroleum Geologists Bulletin 95, 1399–1422.

Treadgold, G., McLain, B., Sinclair, S., Nicklin, D., 2010. Eagle Ford shale Prospecting with 3D seismic data within a tectonic and depositional system framework – Part 1. In: Critical assessment of shale resource plays, AAPG Hedberg Research Conference, Dec., Austin, TX.

Van Wagoner, J.C., Mitchum Jr., R.M., Campion, K.M., Rahmanian, V.D., 1990. Siliciclastic Sequence Stratigraphy in Well Logs, Core, and Outcrops: Concepts for High-resolution Correlation of Time and Facies. In: AAPG Methods in Exploration Series, 7. 55.

Vorce, C.L., Feb. 15, 2011. Interpretation of the Devon Energy Corporation Hull A-102 Conventional Core, Panola Co. TX: Framework for the Haynesville and Bossier Shales. Houston Geol. Soc. Luncheon meeting presentation, Houston.

Zheng, M., 2011. Rock-based characterization of the lower Silurian Longmaxi gas-shale in the southwest Sichuan basin, China, Unpubl.. M.S. thesis, The University of Oklahoma, 126.

Zumberge, J.E., Ferworn, K.J., Curtis, J.B., 2009. Gas character anomalies found in highly productive shale gas wells (abs.): Goldschmidt Conference, Davos, Switzerland, A1539.